# EFFECT OF SITE CITY INTERACION ON THE RESPONSE OF BUILDING USING SURFACE WAVE LOADING

## A DISSERTATION

***Submitted in the partial fulfilment of the requirements for the award of the degree of***

**MASTER OF TECHNOLOGY**

**in**

**EARTHQUAKE ENGINEERING**

**(With Specialization in Seismic Vulnerability & Risk Assessment)**

***by***

**MD JEEESHAN ALI**

**(17553004)**


**DEPARTMENT OF EARTHQUAKE ENGINEERING**
**INDIAN INSTITUTE OF TECHNOLOGY ROORKEE**
**ROORKEE-247 667 (INDIA)**
**JUNE, 2019**

# CANDIDATE'S DECLARATION

I hereby, declare that the work which is being presented in this dissertation entitled, **"EFFECT ON THE RESPONSE OF BUILDING USING SURFACE WAVE LOADING"**, being submitted in partial fulfilment of the requirements for the award of degree of "Master of Technology" in "Earthquake Engineering" with specialization in Seismic Vulnerability & Risk Assessment, to the Department of Earthquake Engineering, Indian Institute of Technology Roorkee, under the supervision of Dr. J.P. NARAYAN Professor, Department of Earthquake Engineering, Indian Institute of Technology Roorkee, is an authentic record of my own work carried out during the period of June 2018 to June 2019.

I declare that I have not submitted the material embodied in this dissertation for the award of any other degree or diploma.

Place: Roorkee
Date:

**MD JEEESHAN ALI**
17553004

# CERTIFICATE

This is to certify that the above statement made by the candidate is correct to the best of my knowledge and belief.

Place: Roorkee
Date:

**(Dr. J.P. NARAYAN)**
Professor
Department of Earthquake Engineering
Indian Institute of Technology Roorkee

# ABSTRACT

This thesis presents a unique research, on what will be the effect on ground motion due to Rayleigh wave generated during the earthquake and to find out what will be the effect on free field ground motion due to the interaction of the Rayleigh wave with structure of the city. And to also find out whether the structure of the city act as a meta-structure for the Rayleigh wave response.

Response of structure constructed on the soft soil is larger and longer duration as compared to structure constructed on stiff rock. Response of free field ground motion is different to that if structure is present on ground due to interaction of structure of city with surrounding earth during seismic event. This thesis presents a study on the effect of Rayleigh wave on response of building and ground motion after crossing the city. Also what will be the role of impedance contrast in site city interaction are studied and to find out weather, structure falling in the path of Rayleigh wave are acting as meta-structure or not. Meta-structure absorbs the energy of Rayleigh wave corresponding to different modes of vibration of building and delays release of energy causing drops in spectra corresponding to different modes of vibration and acting as insulator for the structure falling ahead. For this study, a fourth order accurate viscoelastic FD staggered grid program is used to find out the response of Rayleigh wave for different considered city model of RC and steel building. From this study it is concluded that building types and impedance effect the ground motion and building acting as meta-structure falling in the path of Rayleigh wave and meta-material effect increases with the decrease of impedance contrast. This property helps in designing building in order to have minimum damage during the earthquake.

# ACKNOWLEDGEMENT

First appreciation goes to my parents, without whose beliefs, pursuing post-graduation would still have been a dream.

Completion of this dissertation would not have been possible without the expertise of my supervisor **Dr. J. P. Narayan**, Professor in Department of Earthquake Engineering, Indian institute of Technology Roorkee. Frequent discussions throughout the dissertation work were extremely fruitful and helped me to overcome hurdles and problems I faced during this work.

I am highly obliged to **Dr. Neeraj Kumar**, whose timely help and suggestions accelerated the project work. His sincere guidance, encouragement and proper direction gave insight in learning the modelling and understanding the concept in better way.

I am also thankful to **Mr. Lav Joshi** for their timely help whenever required.

It will be difficult to mention every friend and family members' name but sincere thanks to **Mr. Shailendra Kumar** and **Mr. Vishvendra Tiwari** for their support thorough my journey here.

Thanks to everyone who has helped me achieve this.

# TABLE OF CONTENTS

# LIST OF FIGURES

# LIST OF TABLES

# CHAPTER 1
# INTRODUCTION

## 1.1 General

Nowadays in most of the mega-cities of our country there is continuous increase of number of high-rise buildings and long-span structures. Further, the government of India has planned to develop more than 100 smart cities. Further, the study of Indian seismicity reveals that the most of the occurred earthquakes are shallow in nature. It is now accepted that shallow earthquake generates high frequency Rayleigh waves with large amplitude in its epicentral zone (Narayan and Kumar, 2010). It is also well known that the surface waves are more damaging to both the surface and sub-surface long-span structures as compared to body waves since they can generate large strain in structures in addition to the load reversal. However, till date no emphasis is given to predict the characteristics of Rayleigh waves in research domain and in earthquake resistant designs of long-span structures worldwide.

Further, the seismologists and earthquake engineers bother a lot for the sediment deposit up to depth of 30 m since it amplifies ground motion and brings a drastic change in the ground motion spectral shape. Now, question arise why not to bother for the city in the path of Rayleigh waves with buildings having heights exceeding 30 m and with a high city-density. So, there is an urgent need of quantification of effect of interaction of buildings falling in the path of Rayleigh wave on the characteristics of Rayleigh waves as well as on the response of buildings.

Furthermore, there is also a need of development of seismic meta-materials, so that the damaging Rayleigh waves caused by a very shallow earthquake can be reflected, diverted or mode converted in to the body waves to save a particular structure or a city due to the damaging impact of the Rayleigh waves.

## 1.2 Soil Structure Interaction

The study of soil-structure interaction (SSI) started during 1950's, when Merritt and Housner (1954) studied the SSI effects of 5, 10 and 15 storey buildings on the base shear and fundamental period of the buildings. The ground motions due to earthquake which are not affected by the presence of the structure are called free field motion.

Structure which are constructed on the stiff rock when subjected to the earthquake excitation, then the motion of the surrounding rock is very close to the free field ground motion because of the very high stiffness of the rock structure constructed on the stiff rock can be treated as the fixed base structure. However, when the same structure constructed on the soft soil the responses of the surrounding rock and structure would be very different, because the foundation of the structure could not follow the deformation of the free field motion and also the dynamic response of the structure due to the earthquake excitation affects the deformation of the surrounding soil. Thus, we can define the soil structure interaction as the process in which the responses of the structure and the surrounding soil affect each other. It has been found that effect of SSI on some structure has a very little effect while on some structure its effect is considerable. Effect of neglecting the SSI may result in conservative or non-conservative which depend on the problems and it must be analyzed on a case by case basis. SSI can be classified as two types

a) **Kinematic Interaction:** It is due to the deformation of foundation is different to that of the free field ground motion. The free field ground motion due to earthquake excitation is modified by the rigid foundation which varies over the area around the rigid foundation. It can be analyzed by assuming foundation has no mass.

b) **Inertial Interaction:** Vibration reaching the superstructure through foundation induces inertial forces which develops shear and moment at the base of the foundation which causes further deformation of the surrounding soil.

## 1.3 Site City Interaction

The collective response of the kinematic interaction and inertial interaction is called as site city interaction. The explanation of the behavior of buildings of a city during an earthquake is a great challenge for researchers because of the complex soil-structure interaction. The mass and stiffness play an important role in the dynamic response of a structure and also modify the nearby site response around the structure The first study on site-city-interaction (SCI) effects on the building response and free field motion was carried out by Wirgin and Bard (1996), wherein buildings of the city were used as an equivalent visco-elastic blocks (Bard et al., 2008; Guéguen and Colombi, 2016). The SCI phenomenon is dominant when two conditions are satisfied namely buildings are on soft soil deposit and fundamental frequency of soft soil and building coincides.

Further, the free field motion recorded in the vicinity of structures is alters by seismic waves generated by the structures of the city. Khan et al. (2006) and Semblat et al. (2008) simulated the SH-wave responses of structures situated in a shallow basin under double resonance condition and concluded that the SCI is beneficial to some part of the city (within the city) and detrimental at boundaries of the city. Kumar and Narayan (2018) studied the SCI effects on the response of structures under double resonance condition and reported a drop in response of structures up to 50% as well as the splitting of frequency bandwidth of fundamental mode of vibration of structure due to the SCI effects as compared to a standalone structure (Sahar and Narayan, 2016; Guéguen and Colombi, 2016).

## 1.4 Insulating Effect of City Building

In order to study the effects of interaction of structures of the city with Rayleigh wave on the amplitude of Rayleigh waves in free field, city will be implemented in the FD grid in the form of building blocks between the epicentre and the site of interest (recording station). Kumar (2018) studied the insulating effects of structures of the city on the Rayleigh wave characteristics and reported a considerable decrease of amplitude of Rayleigh waves after crossing the city. So, there is an urgent need of study of insulating effects of different types and numbers of structures on the Rayleigh wave characteristics.

## 1.5 Seismic Metamaterials

Veselago (1968) theoretically investigated a visionary material (meta-material) for electromagnetic waves with simultaneously negative permeability and permittivity. However, after around 30-years, Pendry et al. (1999) demonstrated experimentally that the meta-materials can be developed with a negative refractive index. Colombi et al. (2016a) carried out an experiment in an actual forest environment as well as modeled the Rayleigh wave response of the trees of a forest in a laboratory using thin rods attached to a metallic plate and numerical simulations. Based on the results of numerical simulation, laboratory and field experiment, Colombi et al. (2016b) first time inferred that a densely populated forest can act as a naturally occurring seismic metamaterial for the Rayleigh waves on the geophysical scale. In order to make the structures safe from the damaging high frequency Rayleigh waves caused by shallow earthquakes, there is

an urgent need of development of seismic metamaterials which can deviate, reflect or create band gaps for the Rayleigh wave in a frequency range of 0-5 Hz.

# CHAPTER 2

# SALIENT FEATURES OF THE USED FINITE-DIFFERENCE PROGRAM

## 2.1 General

The fourth-order accurate staggered-grid finite-difference (FD) method is one of the most popular numerical methods for the simulation of seismic wave propagation (Madariaga, 1976; Graves, 1996; Pitarka, 1999; Kristek and Moczo, 2003; Narayan and Kumar, 2014; Narayan and Sahar, 2014). A frequency dependent damping in the time domain FD simulation of site-city-interaction effects on the building response and free field motion is essential in order to explain the transfer function of the buildings (Narayan and Kumar, 2013). In the past, very simple approaches were used to incorporate the damping in time-domain simulations due to non-availability of requirement computational memory and time (Narayan and Kumar, 2008). However, Day and Minster (1984) first time attempted to incorporate the realistic viscoelastic damping into a 2D time-domain FD algorithm based on Padé approximation. Emmerich and Korn (1987) improved the incorporation of viscoelastic damping in time domain simulation using a rheological model widely known as generalized Maxwell body (GMB-EK model) for the earth material. Kristek and Moczo (2003) introduced material independent anelastic function which is better one in case of material discontinuity in the FD grid.

The used P-SV wave fourth-order spatial accurate staggered-grid viscoelastic FD program is developed by Narayan and Kumar (2014). The program has used viscoelastic P-SV wave equations which are based on GMB-EK rheological model and material independent anelastic function (Emmerich and Korn, 1987; Kristek and Moczo, 2003). The viscoelastic P-SV wave equations based on GMB-EK rheological model are given below,

$$\rho \frac{\partial U}{\partial t} = \frac{\partial \sigma_{xx}}{\partial x} + \frac{\partial \sigma_{xz}}{\partial z} \tag{2.1}$$

$$\rho \frac{\partial W}{\partial t} = \frac{\partial \sigma_{xz}}{\partial x} + \frac{\partial \sigma_{zz}}{\partial z} \tag{2.2}$$

$$\frac{\partial \sigma_{xx}}{\partial t} = \overline{K_u}\left(\frac{\partial U}{\partial x}\right) + \overline{\lambda_u}\left(\frac{\partial W}{\partial z}\right) - \sum_{l=1}^{m}\left[\overline{Y_l^{\alpha}}\left(\chi_l^{xx}\right) + \overline{Y}_l^{\lambda}\left(\chi_l^{zz}\right)\right] \quad (2.3)$$

$$\frac{\partial \sigma_{zz}}{\partial t} = \overline{K_u}\left(\frac{\partial W}{\partial z}\right) + \overline{\lambda_u}\left(\frac{\partial U}{\partial x}\right) - \sum_{l=1}^{m}\left[\overline{Y_l^{\alpha}}\left(\chi_l^{zz}\right) + \overline{Y}_l^{\lambda}\left(\chi_l^{xx}\right)\right] \quad (2.4)$$

$$\frac{\partial \sigma_{xz}}{\partial t} = \overline{\mu_u}\left[\left(\frac{\partial U}{\partial z}\right) + \left(\frac{\partial W}{\partial x}\right)\right] - \sum_{l=1}^{m}\left[\overline{Y}_l^{\mu}\left(\chi_l^{xz}\right)\right] \qquad l=1,2,,, m \quad (2.5)$$

Where U and W are the particle velocity components in the X and Z-directions, respectively. $\sigma_{xx}$, $\sigma_{zz}$ and $\sigma_{xz}$ are the normal and shear stress components and ρ is the density. $\bar{K}_u$, $\bar{\lambda}_u$ and $\bar{\mu}_u$ are the modified unrelaxed elastic parameters and $\bar{Y}_l^{\alpha}$, $\bar{Y}_l^{\lambda}$ and $\bar{Y}_l^{\mu}$ are the modified anelatic coefficients. $\chi_l^{xx}$, $\chi_l^{zz}$ and $\chi_l^{xz}$ are the anelastic functions and $\frac{\partial}{\partial x}, \frac{\partial}{\partial z} and \frac{\partial}{\partial t}$ are the differential operators. 'm' is the number of relaxation frequency.

Further, the required unrelaxed elastic parameters $K_u$ and $\mu_u$ for P-wave ($K_u$) and S-wave ($\mu_u$) respectively have been obtained using phase velocity of P-wave ($V_{P,\omega_r}$) and S-wave ($V_{S,\omega_r}$) at reference frequency ($\omega_r$) and the following equations (Moczo et al., 1997).

$$\mu_u = \rho V_{S,w_r}^2 \frac{R+\vartheta_1}{2R^2} \qquad \text{Where } R = \sqrt{\vartheta_1^2 + \vartheta_2^2} \quad (2.6)$$

$$K_u = \rho V_{P,w_r}^2 \frac{R+\vartheta_1}{2R^2} \qquad \text{Where } R = \sqrt{\vartheta_1^2 + \vartheta_2^2} \quad (2.7)$$

$$\vartheta_1 = 1 - \sum_{l=1}^{n}\left[Y_l \frac{1}{1+\left({}^{\omega_r}/_{\omega_l}\right)^2}\right] \quad \vartheta_2 = \sum_{l=1}^{n}\left[Y_l \frac{{}^{\omega_r}/_{\omega_l}}{1+\left({}^{\omega_r}/_{\omega_l}\right)^2}\right] \qquad l = 1,2,,m \quad (2.8)$$

In case of P-wave $Y_l$ will be replaced by $Y_l^{\alpha}$ and that in case of S-wave will be replaced by $Y_l^{\mu}$ in equation (8). The unrelaxed Lame's parameter $\lambda_u$ is obtained using the following relationship:

$$\lambda_u = K_u - 2\mu_u \quad (2.9)$$

The anelastic coefficients $Y_l^{\lambda}$, $l = 1, 2, \ldots, m$ were obtained using the following relationship:

$$Y_l^{\lambda} = \frac{K_u Y_l^{\alpha} - 2\mu_u Y_l^{\mu}}{\lambda_u} \quad (2.10)$$

At the free surface stress imaging technique used as a free surface boundary condition (Graves 1996; Narayan and Kumar, 2008). The sponge boundary proposed by Israeli and Orszag (1981) is implemented on the model edges to avoid the edge reflections (Narayan and Kumar, 2008).

## 2.2 Model discretization and source implementation

The model is discretized with the grid size of 3m in horizontal direction while in vertical direction grid size of 3m is taken up to a depth of 1500m, after that grid size is taken 6m. A city model consists of 30 building of equal width and height. The distance of first block from the focus is 3.3Km and recording station is at a distance of 5.5 Km as shown in figure 3.1 showing brief sketch of city model. For the simulation of Rayleigh wave responses of a city, a fourth-order accurate P-SV wave staggered grid viscoelastic FD program developed by the Narayan and Kumar (2014) is used. To incorporate the real buildings in FD grid a homogenous viscoelastic building blocks of 5% and 2% damping for Reinforce concrete (RC) and steel building is used in place of real RC-building and steel building as proposed by Bard (2005) and Sahar et al. (2015). Time step is taken for satisfying the stability criteria for fourth order accurate staggered accurate FD program according to the equation given below:

$$\frac{V_{\max} \times \Delta t}{\min(\Delta x or \Delta z)} = 0.606 \tag{2.11}$$

A point source dominated by the SV-wave is generated in the FD grid by applying a shear stress $\sigma_{xz}$ in the form of Gabor wavelet with dominant frequency 2.0 Hz at a focal depth of 120 m. The frequency bandwidth for the Gabor wavelet corresponding to dominant frequency 2.0 Hz is 0-6 Hz. The interaction of the incident SV-wave at the free surface at the critical distance resulted in the generation of the evanescence P-wave and the reflected SV-wave. Now, the coupling of the evanescence P-wave and the reflected SV-wave is responsible for the generation of Rayleigh wave (Narayan and Kumar, 2010). Mathematical equation for Gabor wavelet used for the generation of Rayleigh wave is shown below:

$$S(t) = e^{-\alpha}.\cos[\omega p(t - ts) + \phi] \tag{2.12}$$

Where $\alpha = \frac{\omega p(t-ts)^2}{\Upsilon}$, $f_p$ is predominant frequency, $\Upsilon$ controls the oscillatory character, $t_s$ controls the duration of wavelet and $\phi$ is the phase shift. Figure 2.1 shows the

generated Gabor wavelet & corresponding spectra for $f_p$ = 2Hz, ϒ= 0.5, $t_s$ = 1.5 and ϕ=0. The frequency bandwidth of the generated Gabor wavelet is 0- 8.0 Hz.

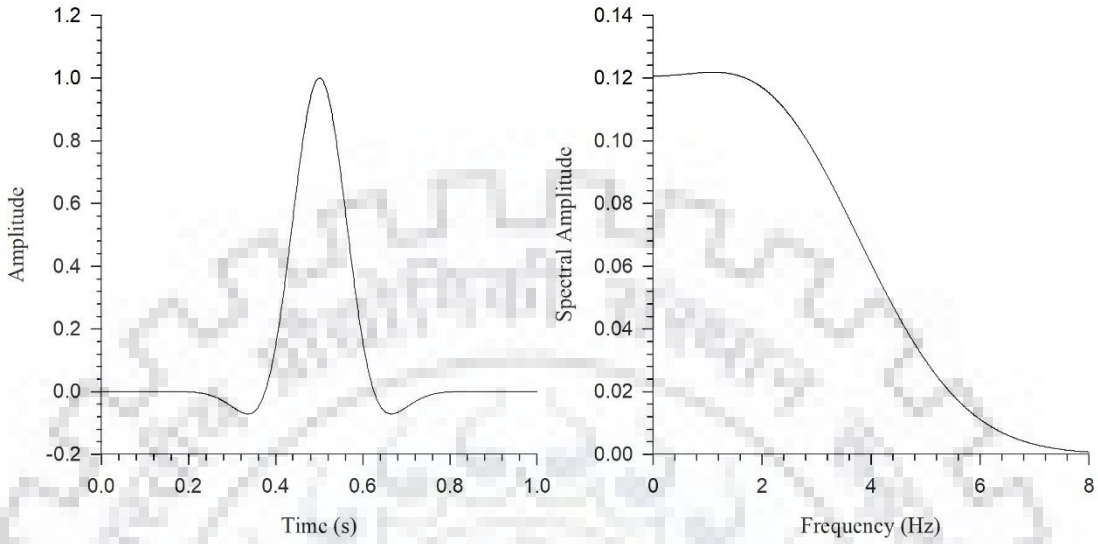


**Figure 2.1** Gabor wavelet in time domain and its spectra

## 2.3 Validity of FD program

As we all know that the velocity of seismic wave is higher in stiff media as compared to media and when a soil deposit present above the stiff rock, wave travelling from stiff rock to deposits, wave increases it amplitude in order to conserve its energy. So in order to verify that the various results obtained using FD program, which are accurate or not, response of SH wave are obtained for the rock are obtained in the presence and absence of soil deposits of thickness 36m. Due to the presence of loose soil deposits, amplification of SH wave occurs at their fundamental frequency which is obtained by a simple equation given below:

$$F_o = \frac{V_s}{4H} \tag{2.12}$$

Where,

$F_o$ =fundamental frequency of soil deposits,

H=thickness of soil deposits

$V_s$ =shear wave velocity in soil deposits.

The parameters of rocks and loose soil deposits used for the simulation of SH wave using FD program to obtain the amplification of SH wave due presence of soil deposits are given in Table 2.1.

A SH wave is generated using a Gabor wavelet of dominant frequency 1 Hz at the depth of 160m using a line source.

**Table 2.1** Parameters of Rock and Soil Deposits

| Medium | S-wave velocity ($V_s$) | Quality factor (Q) | Density ($Kg/m^3$) | Impedance |
|---|---|---|---|---|
| Soil deposits | 400 | 40 | 2000 | 80000 |
| Rock | 2200 | 220 | 2800 | 616000 |

Spectral amplification due to the presence of loose soil deposits can also be obtained by empirical equation given below:

$$A = \frac{1}{\frac{1}{IC} + 0.5\pi\xi} \tag{2.13}$$

Where,

IC=Impedance contrast

A=Amplification

$\xi$ =Damping

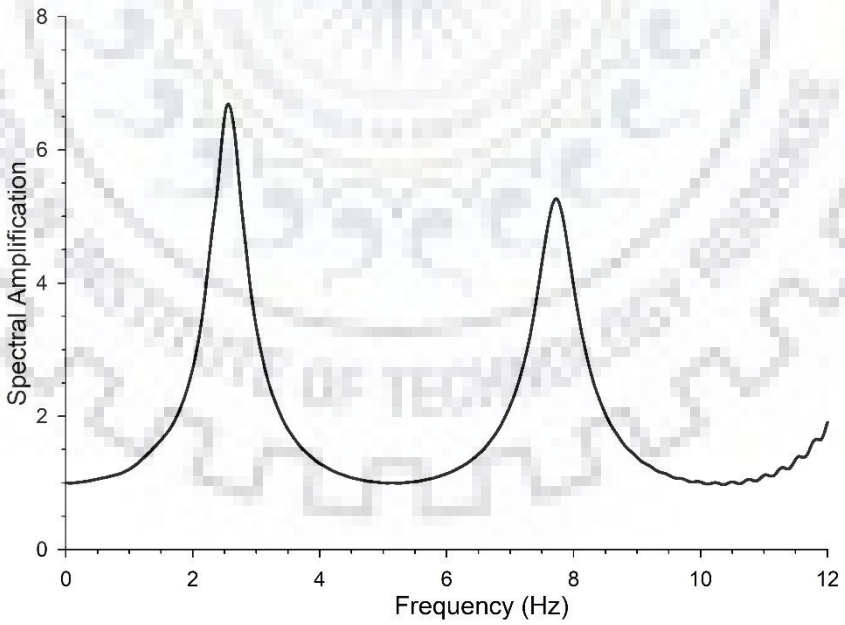


**Figure 2.2** Spectral amplification of SH wave

The comparison of amplification obtained using FD simulation and empirical equation are given in Table 2.2.

**Table 2.2** Comparison of Simulation and Empirical Equation Result for Amplification and Fundamental Frequency

| Type | Fundamental Frequency (Hz) | Amplification |
|---|---|---|
| FD Simulation | 2.53 | 6.53 |
| Empirical Equation | 2.78 | 6.87 |

Table 2.2 shows that there is excellent match of amplification and fundamental frequency obtained using FD simulation and empirical equation, and its infers that the FD program used for the simulation of various models are accurate.

# CHAPTER 3
# ANALYSIS OF RAYLEIGH WAVE INTERACTION WITH CITY MADE-UP OF STEEL-BUILDINGS

## 3.1 Introduction

There is day by day an increase of number of structures everywhere in India and this increase is more in the mega-cities. Now, question arises whether there is any cumulative effect of such structures on the characteristics of Rayleigh wave caused by shallow earthquakes. We bother a lot for the sediment deposit up to depth of 30 m since it amplifies ground motion and brings a drastic change in the spectral shape of ground motion. It is now documented that shallow earthquakes generate high frequency Rayleigh waves with large amplitude in their epicentral zone (Narayan and Kumar, 2010). Further, such Rayleigh waves may be more damaging to both the surface and sub-surface long-span structures as compared to body waves since they can generate large strain in structures in addition to the load reversal. However, till date no emphasis is given to predict the characteristics of Rayleigh waves in research domain and in earthquake resistant designs of long-span structures worldwide.

Further, there is need of development of seismic metamaterials which can reflect, convert in to body waves or redirect the Rayleigh waves so that a particular city or a structure can be saved from the damaging effects of the Rayleigh waves. The metamaterial is a theoretical concept proposed by the Veselago in 1968, as this material develops a simultaneous negative permeability and permittivity for the electromagnetic waves. Pendry et al. (1999) showed experimentally that it is possible to develop a material with the negative refractive index. A metamaterial has a property of manipulating the waves by absorbing, bending, enhancing or by blocking the wave to achieve the desired effect which is beyond the natural material. Such metamaterials have been extensively used in the field of optics, electromagnetism, semiconductor engineering and nano-science. A seismic metamaterial is a composite medium made up of group of sub-wavelength resonators. The physical phenomenon like Bragg's scattering and Fano resonance are responsible for the dips in the spectra corresponding to their frequency and create a band-gap. Fano resonance is a combined effect of

background scattering and resonance scattering and dips in the spectra is due to resonance scattering as explained by Goffaux et al. (2002). Tsakmakidis (2007) and Colombi et al. (2016) found that in the case of Fano resonance the dips in the spectra match with the fundamental frequency of the sub-wavelength resonators. These resonators absorb the energy of a wave corresponding to their fundamental frequency and release the energy with certain delay.

The role of impedance contrast between the building blocks of the city and the underlying earth material in the insulating effects of structures on the characteristics of the Rayleigh waves as well as to infer whether a building block can act as a metamaterial for the Rayleigh waves are studied in details and documented in this chapter.

## 3.2 Model Parameters

In order to study the effects of interaction of Rayleigh waves with the Steel-buildings of the city on the characteristics of Rayleigh wave as well as on the response of building itself, we have to incorporate the Steel-buildings of the city in the FD grid. Incorporation of structures of the city in the FD grid is impossible at present due to the lack of computational memory and speed. Therefore, scientists have used building blocks in place of structures of a city and making sure that the weight, dimension and different modes of vibrations of a building block matches with that of the real Steel-building (Bard at el, 2005; 2008; Sahar at el. 2015; Sahar and Narayan, 2016).

Section used in the present study for column, beam is ISHB400 and ISMB300. The distance between the column is taken as 5m and height of column as 3m. The plan of steel building is taken as 45m by 45m having height of 65m. The thickness of concrete slab and masonry wall of density 2500Kg/$m^3$ and 1900 Kg/$m^3$ are 150mm and 230mm respectively. The live load taken as 4KN/$m^3$. The effective density of steel building block can be obtained by using all the weight of beam column, slab, wall and live load which is coming out to be 350 Kg/$m^3$ the shear velocity in Steel building is taken as 160 m/s based on the analysis of (Clotaire & Philippe Gueguen). For a pilot study, the considered velocity of S-Wave and P-Wave for building block and surrounding material along with the quality factor and unrelaxed moduli of rigidity is given in Table 3.1. Quality factor is inversely related to damping which is coming out to be 25 for 2% damping for steel building. The quality factor for surrounding material is

taken as 10 % of the considered velocity. The inelastic parameter of building block and surrounding material corresponding to $\mu_u$, $\lambda_u$ and $K_u$ is given is given in Table 3.2

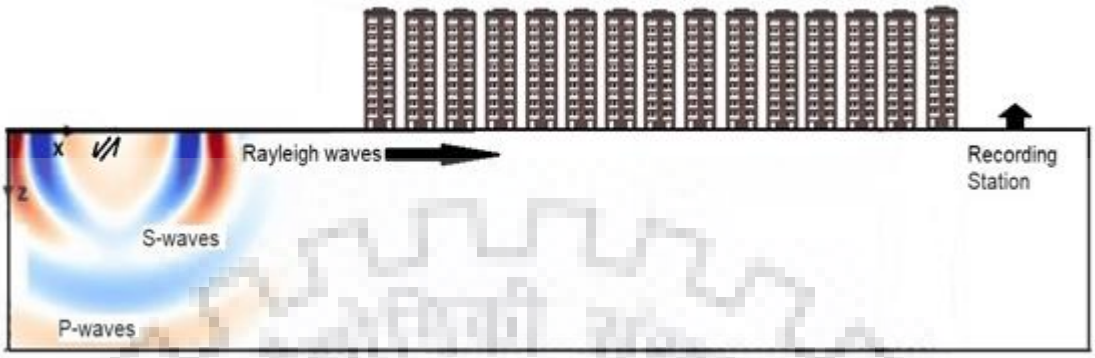


**Figure 3.1** Sketch showing interaction of the Rayleigh wave with the steel-buildings of a city

**Table 3.1** Rheological Parameters of Building Blocks and Surrounding Rock.

| Material | Velocity (m/s) | | Quality Factor | | Density (kg/m$^3$) | Unrelaxed Moduli (GPa) | | |
|---|---|---|---|---|---|---|---|---|
| | $V_P$ | $V_s$ | $Q_P$ | $Q_S$ | | $\mu_u$ | $K_u$ | $\lambda_u$ |
| Blocks | 280 | 160 | 25 | 25 | 350 | 0.009 | 0.026 | 0.006 |
| Rock | 1720 | 700 | 172 | 72 | 1450 | 0.735 | 0.900 | -0.571 |

**Table 3.2** Inelastic Parameters of Building Blocks and Rock

| Building Blocks | | | Rock | | |
|---|---|---|---|---|---|
| $\mu_u$ | $\lambda_u$ | $K_u$ | $\mu_u$ | $\lambda_u$ | $K_u$ |
| 0.051 | 0.051 | 0.051 | 0.022 | -0.013 | 0.009 |
| 0.048 | 0.048 | 0.048 | 0.019 | -0.013 | 0.008 |
| 0.051 | 0.052 | 0.052 | 0.019 | -0.015 | 0.008 |
| 0.069 | 0.069 | 0.069 | 0.025 | -0.022 | 0.010 |

## 3.3 Rayleigh wave response of homogeneous half space model

In order to quantify the insulating and meta-material effects of the steel-buildings of the city on the response of steel-building itself and the free field motion, there is need of Rayleigh wave response of homogeneous half-space model as a reference one. The rheological parameters of the homogeneous half-space model are the same as given in Table 3.1. Figure 3.1(a) shows the horizontal and vertical component of seismic

response of homogeneous half-space model at 15 equidistant recording stations spaced at 144m. The incident P-wave, evanescence P-wave, incident SV-wave is not visible in figure 3.2(a) because of normalization of the traces in both the components. However, Rayleigh waves are prominently visible in Figure 3.2(a). Further, the amplitude of Rayleigh wave in the vertical component is larger than in the horizontal component. The decrease of amplitude of Rayleigh wave with the epicentral distance seems negligible due to the non-occurrence of the divergence effect. The divergence effect is not occurring in the 2D simulation since a cross section of the cylindrical wave front of Rayleigh wave is propagating as a line with a fixed length in the vertical direction. There is damping only which is responsible for the minor decrease of amplitude of Rayleigh wave with the distance travelled in the XZ-plane.

Figure 3.2(b) and (c) shows the spectra of horizontal and vertical components of Rayleigh wave part only at an epicentral distance of 3400 m and 5500 m, respectively. Figure 3.2 clearly reveals that the frequency content in the generated Rayleigh wave is in a frequency band 0-6 Hz. Further, a frequency dependent damping can be observed. There is a decrease of spectral amplitude as per frequency and change in the spectra of Rayleigh wave after travelling a distance of 2100 m.

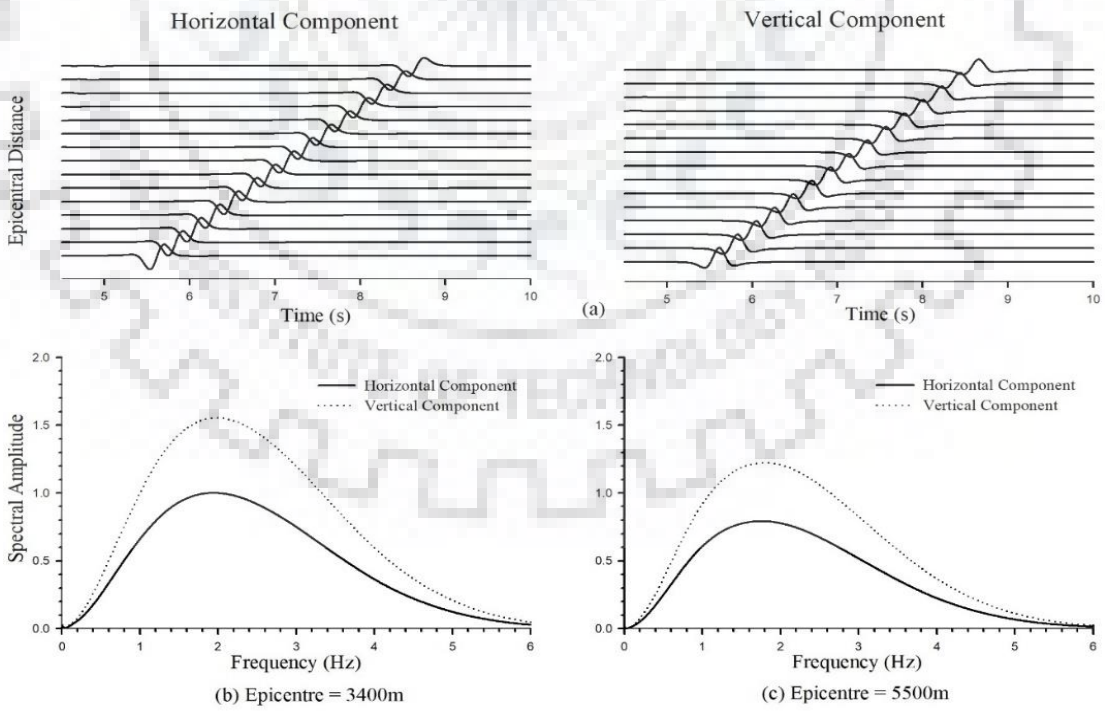


**Figure 3.2**(a) Horizontal & vertical component of Rayleigh wave, (b) and (c) spectra of Rayleigh wave

## 3.4 Interaction of the Rayleigh wave the steel buildings of a City: A Pilot Study

In order to infer the cumulative effects of interaction of Rayleigh wave with the individual steel-building of the city on the response of steel-building itself as well as on the characteristics of the Rayleigh wave after crossing the city, the seismic response of a city made up of 30 steel-buildings with width and height 30m and 45m respectively, computed at the top of the buildings and at the free surface at an epicentral distance of 3300m.

### 3.4.1 Response of steel buildings

Figure 3.3 (a) depicts a comparison of horizontal and vertical components of response of S1-building with the free field motion at the same location. In the case of horizontal component, there is drastic increase of duration of motion at the top of S1-building as compared to the free field motion at that location, but there is only minor increase in amplitude as compared to the free field motion. On the other hand, in the case of vertical component, there is drastic increase of both the amplitude and duration of motion at the top of S1-building as compared to the free field motion. As per physics, the waves cannot propagate in the building block. So, whatever we have recorded on the top of the structures are the guided SV-wave and P-wave.

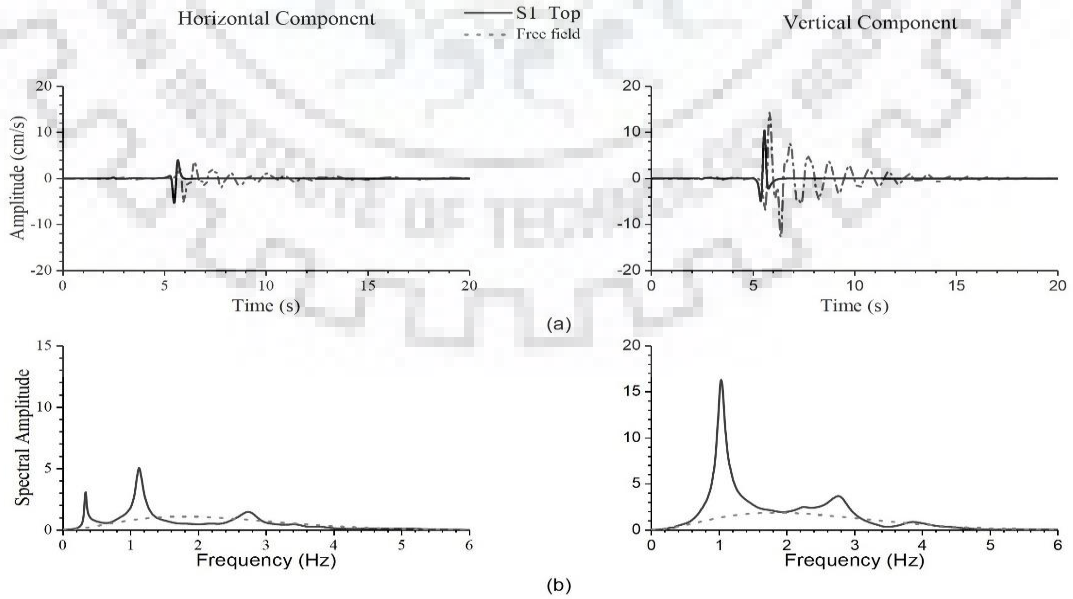


**Figure 3.3** (a) Comparison of response at top of S1 building with free field (b) comparison of spectra at top with free field

The left and right panels of Figure 3.3 (b) shows the comparison of spectral of the horizontal (left panel) and vertical components (right panel) of response of S1 steel building with the free field motion. An analysis of Figure 3.3(b) depicts spectral peaks at discrete frequencies in both the components. In order to infer and match these spectral peak frequencies with the fundamental flexural and longitudinal modes of vibrations of the building block, the fundamental flexural ($SVF^{S}_{O2D}$) and longitudinal ($PF^{S}_{O2D}$) modes of vibration for the SV-wave and P-wave, respectively were computed using equations given by Kumar and Narayan (2018).

$$\frac{SVF^{S}_{02D}}{F^{S}_{01D}} = \left[\frac{\left\{3-\left(\frac{H}{W}\right)\right\}}{3.2}\right] \tag{3.1}$$

$$PF^{S}_{02D} = \frac{V_P}{4H} \tag{3.2}$$

$$F^{S}_{01D} = \frac{V_S}{4H}, V_P = \sqrt{\frac{E}{\rho}} \tag{3.3}$$

Where,

H=Height of block

W=Width of block

$SVF_{02D}$= fundamental flexural frequency of building block in 2D

$F_{01D}$= 1D fundamental frequency of building block

$PF_{02D}$= 2D fundamental longitudinal frequency of building block

$V_P$= velocity of P-wave in building block.

$V_S$= shear wave velocity in building block.

E=young modulus of building block

$\rho$ =density of building block

E = Young's modulus of building block

A comparison of numerically obtained fundamental flexural and longitudinal frequencies of the building block with those computed using empirical equations of Kumar and Narayan (2018) is given in Table 3.3. An analysis of Table 3.3 depicts an excellent match of the numerically obtained fundamental flexural and longitudinal frequencies of the building block with those computed empirically given by Kumar and Narayan (2018).

**Table 3.3** Comparison of Computed & Simulated Fundamental Flexural and Longitudinal Frequency of the Building Block

| S.No. | Component | FD Simulation | Empirical relation |
|---|---|---|---|
| 1 | $SVF_{02D}^{S}$ | 0.33 Hz | 0.31 Hz |
| 2 | $PF_{02D}^{S}$ | 1.12 Hz | 1.14 Hz |

### 3.4.2 Response at the free field recorder

The left and right panels of figure 3.4 (a) show the comparison of horizontal (left panel) and vertical component (right panel) of the response of the site-city model at the recording station with that in the absence of the city. A decrease of the Rayleigh wave amplitude after crossing the city can be inferred. There is around 17% and 19% decrease of amplitude of Rayleigh wave in the horizontal and vertical components after interacting with the 30 steel-building of the city. There is an increase of duration of ground motion in the case of response of the city. These extra phases may be due to the vibrations of the individual steel-buildings of the city. The vibrating structures may release their energy to the earth in the form of body and the surface waves. Similarly, the left and right panels of Figure 3.4 (b) show the comparison of spectra of the horizontal (left panel) and vertical components (right panel) of the response of the site-city model at the recording station with those in the absence of city. An analysis of figure 3.4 (b) shows drops in the spectra corresponding to the different modes of the flexural and longitudinal vibrations of the building blocks. These drops may be arising due to the phase difference (out of phase) of $\pi$ between the waves released by the building blocks as compared to the free field ground motion in the absence of city.

The left and right panels of Figure 3.4 (c) show the spectral ratio of the horizontal (left panel) and vertical components (right panel) of the free field motion corresponding to with and without city in the model. An analysis of Figure 3.4 (c) shows spectral ratio drops corresponding to the different modes of flexural and longitudinal vibrations of the building blocks. These spectral ratio drops may be arising due to the phase difference of $\pi$ between the waves released by the building blocks as compared to the free field ground motion in absence of the city. The value of spectral ratio drop corresponding to the fundamental longitudinal mode of vibration of building blocks is the largest one. On the other hand, the value of spectral ratio drop corresponding to the flexural fundamental mode of vibration of building blocks is too less as compared to the

fundamental longitudinal mode of vibration. Further, considerable spectral ratio drops corresponding to the higher longitudinal modes of vibrations of the building block can be inferred in both the components of the Rayleigh wave. It is interesting to note that the observed different spectral ratio drops are same in both the components of the Rayleigh wave.

Figure 3.4 (c) also reveals a continuous decrease in the spectral amplitude of Rayleigh in both the horizontal and vertical components of Rayleigh wave with the increasing frequency. This may be due to the background scattering of the Rayleigh wave during the interaction of the Steel-buildings. From the above result, it is inferred that the steel-buildings of city are acting as an insulator for the Rayleigh wave as well as a sub-wavelength resonator.

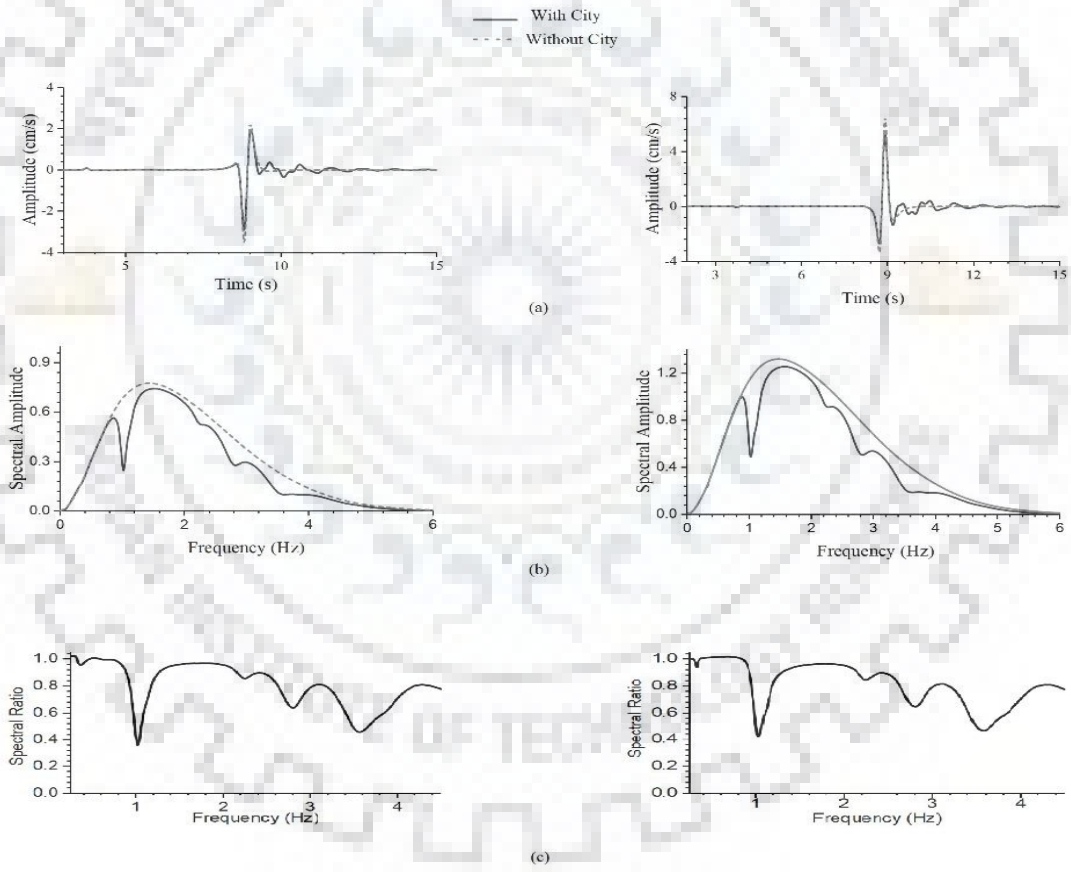


**Figure 3.4** (a) A comparison of responses of Rayleigh wave at station (b) A comparison of spectra (c) Comparison of spectral ratios

## 3.5 Role of impedance contrast in insulating effect of Steel buildings

### 3.5.1 Insulating effects on free field motion

To study the role of impedance contrast between the building blocks and the underlying earth material in the insulating effects of buildings on the characteristics of the Rayleigh wave, the Rayleigh wave responses of the various site-city models with the same source parameters as well as the numbers of buildings and the rheological parameters of the building blocks but with a varying impedance in the homogeneous half-space were computed and analyzed. For this study, five-different impedance contrast models namely ICSB1, ICSB2, ICSB3, ICSB4 and ICSB5 with different impedance in homogeneous half-space rock are taken whose rheological parameters are given in the table 3.4 and their corresponding inelastic parameters are given in Table 3.5

**Table 3.4** Rheological Parameter of the Half-Space in the ICSB1 to ICSB5 Impedance Contrast Models (Parameters of Building Blocks are same as given in Table 3.1)

| IC models | Velocity (m/s) | | Quality factor (Q) | | Density (kg/m$^3$) | IC for S-wave | Unrelaxed moduli (GPa) | | |
|---|---|---|---|---|---|---|---|---|---|
| | $V_P$ | $V_s$ | $Q_P$ | $Q_S$ | | | $\mu_u$ | $K_u$ | $\lambda_u$ |
| ICSB1 | 700 | 350 | 70 | 35 | 1200 | 10.00 | 0.157 | 0.152 | -0.163 |
| ICSB2 | 1720 | 700 | 172 | 70 | 1450 | 24.17 | 0.735 | 0.900 | -0.571 |
| ICSB3 | 2200 | 1050 | 220 | 105 | 1700 | 42.50 | 1.918 | 1.467 | -2.365 |
| ICSB4 | 2615 | 1400 | 262 | 140 | 1950 | 65.00 | 3.889 | 2.070 | -5.707 |
| ICSB5 | 3100 | 1750 | 310 | 175 | 2200 | 91.67 | 6.832 | 2.905 | -10.758 |

**Table 3.5** Inelastic Parameters of Surrounding Homogeneous of Surrounding Rock (Inelastic Parameters of Building Block is same as in Table 3.2)

| Model | $\mu_u$ | $\lambda_u$ | $K_u$ |
|---|---|---|---|
| ICSB1 | 0.03974669 | -0.0101144 | 0.022083598 |
| | 0.036188727 | -0.01323824 | 0.019301534 |
| | 0.038044929 | -0.01739541 | 0.019792335 |
| | 0.049455655 | -0.02936735 | 0.024639149 |
| ICSB2 | 0.022083598 | -0.01325117 | 0.009566398 |
| | 0.019301534 | -0.01331519 | 0.008157722 |
| | 0.019792335 | -0.01529167 | 0.008241645 |
| | 0.024639149 | -0.02184897 | 0.010002907 |
| ICSB3 | 0.015248292 | -0.00648502 | 0.007549355 |
| | 0.013144519 | -0.00655553 | 0.006413811 |
| | 0.013366622 | -0.00759527 | 0.006465348 |
| | 0.016403894 | -0.0108688 | 0.007817404 |
| ICSB4 | 0.011638556 | -0.0034632 | 0.006396973 |
| | 0.009963394 | 0.000895159 | 0.006865145 |
| | 0.010089443 | -0.00131428 | 0.006335002 |
| | 0.012294237 | -0.00179562 | 0.00785821 |
| ICSB5 | 0.009409305 | -0.00188061 | 0.005409897 |
| | 0.008021421 | -0.00205596 | 0.004578389 |
| | 0.00810252 | -0.00252244 | 0.004604471 |
| | 0.00983113 | -0.00378087 | 0.005545549 |

The left panels of Figure 3.5(a) to (e) show a comparison of the horizontal component of the Rayleigh wave responses of the ICSB1 to ICSB5 site-city models corresponding to with and without city in the model at the recording station. Similarly, the right panels of Figure 3.5 show a comparison of spectra of the horizontal component of the Rayleigh wave responses of the ICSB1 to ICSB5 site-city models corresponding to with and without city in the model at the recording station. The decrease of amplitude of Rayleigh wave and corresponding spectra in both the responses (with and without the city in the model) with an increase of impedance in the homogeneous half-space is due to the use of a fixed stress drop in source time function (Gabor wavelet) in all the ICSB1 to ICSB5 site-city models to generate the point source.

The analysis of Figure 3.5 reveals that as the impedance contrast between the steel-buildings and the underlying half-space is decreasing the amplitude decrease due to the insulating effects of steel-buildings is increasing. Table 3.6 shows the amplitude of Rayleigh wave corresponding to without and with city in the model and the % decrease of amplitude of the Rayleigh waves due to the insulating effects of Steel-buildings. For example, the % amplitude decrease of the Rayleigh wave in the horizontal component are 39.40%, 17.66%, 10.13%, 6.40% and 4.37% in the ICSB1 to ICSB5 site-city models, respectively. Further, there is an increase of value of drops in the spectra of the horizontal components of Rayleigh wave corresponding to different modes of flexural and longitudinal vibrations of the steel-buildings with the decrease of impedance contrast. So, it can be inferred that there is an increase of insulating effects of the steel-buildings with a decrease of impedance contrast between the building blocks and the underlying half-space.

Similarly, the upper panels of Figure 3.7 illustrate the comparison of spectral ratio drops in the horizontal components of Rayleigh wave corresponding to the ICSB1 to ICSB5 site-city models. The spectral ratio drops corresponding to the certain discreet frequencies are increasing with decrease of impedance contrast between building blocks and the underlying half-space. However, there is no change of frequency corresponding to these spectral ratio drops with decrease of IC. But it is interesting to note that the width of the spectral ratio drops is increasing with the decrease of IC and increase of frequency to some extent. This effect is clearly visible in the case of ICSB1 site-city model where IC is 10 and there is band gap between 3.5 to 4.0 Hz.

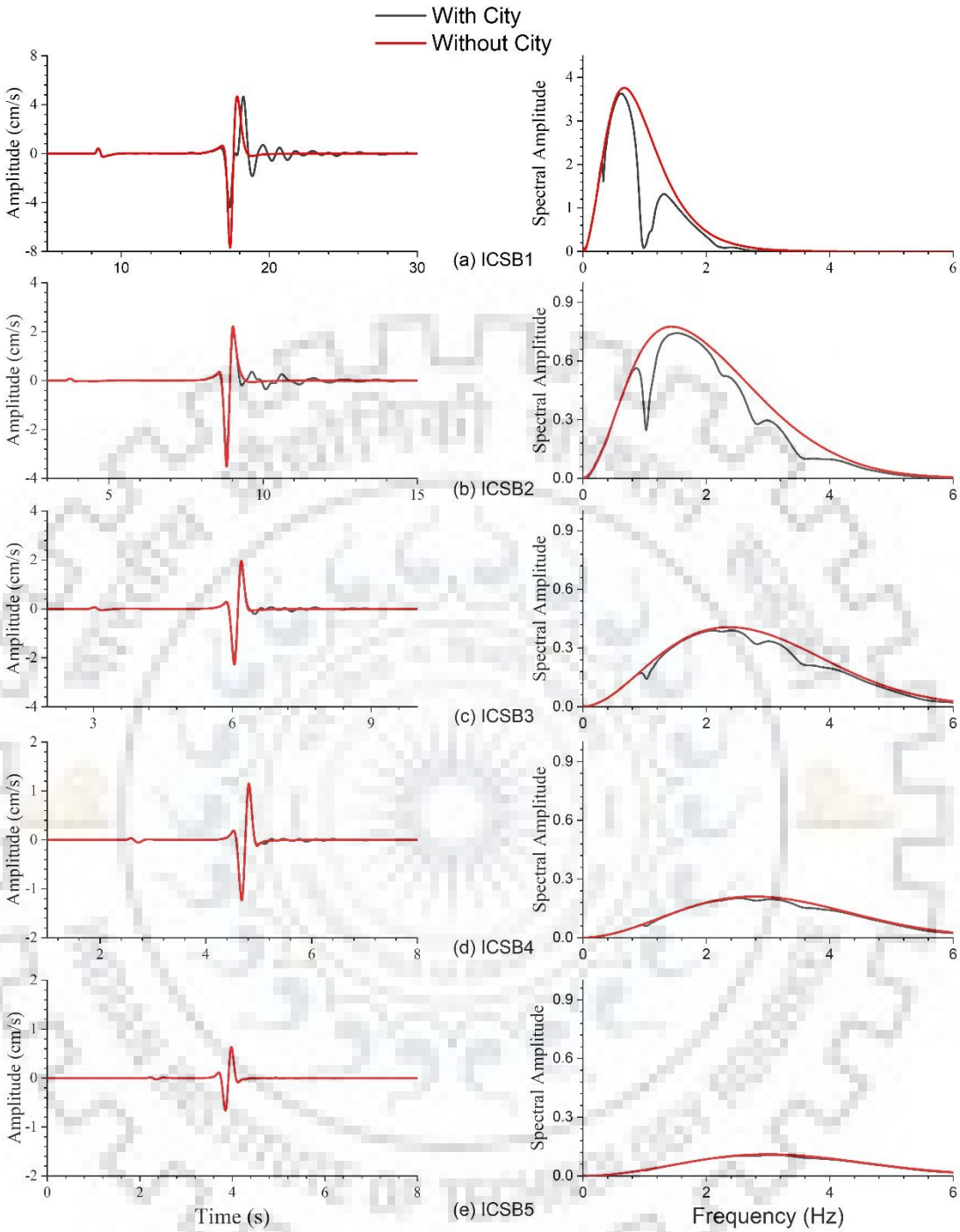


**Figure 3.5**(a) to (e) Comparison of the horizontal components of the Rayleigh wave response (left panels) and spectra (right panels) at station

**Table 3.6** Peak Ground Velocity (PGV) at the Recording Station in the Presence and Absence of the City for both the Components of the Rayleigh Wave

| Model | Horizontal component (PGV)(cm/s) | | | Vertical component (PGV)(cm/s) | | |
|---|---|---|---|---|---|---|
| | With city | Without city | % Decrease | With city | Without city | % Decrease |
| ICSB1 | 4.66 | 7.69 | 39.42 | 5.96 | 12.76 | 53.32 |
| ICSB2 | 2.89 | 3.51 | 17.66 | 5.35 | 6.65 | 19.43 |
| ICSB3 | 2.04 | 2.27 | 10.13 | 3.97 | 4.43 | 10.36 |
| ICSB4 | 1.15 | 1.23 | 6.40 | 2.16 | 2.32 | 6.68 |
| ICSB5 | 0.634 | 0.66 | 4.37 | 1.15 | 1.20 | 4.20 |

Similarly, the left panels of Figure 3.6 (a) to (e) show a comparison of vertical component of the Rayleigh wave responses of the ICSB1 to ICSB5 city-models corresponding to with and without city in the model at the recording station. The right panels of Figure 3.6 show a comparison of spectra of the vertical component of the Rayleigh wave responses of the ICSB1 to ICSB5 site-city models corresponding to with and without city in the model at the recording station. The decrease of amplitude of Rayleigh wave and corresponding spectra in both the responses (with and without the city in the model) with an increase of impedance in the homogeneous half-space is due to the use of a fixed stress drop in source time function (Gabor wavelet) in all the ICSB1 to ICSB5 models to generate the point source, as was observed in the case of horizontal components. The analysis of Figure 3.6 reveals that as the impedance contrast between the building block and the underlying half-space is decreasing the amplitude of Rayleigh in the vertical component decreases due to the increase of insulating effects of buildings. Table 3.6 shows the amplitude of Rayleigh wave in the vertical components corresponding to without and with city in the model and the % decrease of the amplitude of the Rayleigh wave in the vertical component due to the insulating effects of building blocks. For example, the % decrease of amplitude of the Rayleigh wave in the vertical component are 53.32%, 19.43%, 10.36%, 6.68% and 4.20% in the ICSB1 to ICSB5 site-city models, respectively. Further, there is also an increase of value of drops in the spectra of vertical components corresponding to different modes of flexural and longitudinal vibrations of the buildings with the decrease of impedance contrast. So, it can be inferred that there is an increase of

insulating effects of building blocks with a decrease of IC between the building blocks and the underlying half-space.

The lower panel of Figure 3.7 illustrates the comparison of spectral ratio drops in the vertical components of the Rayleigh waves corresponding to the ICSB1 to ICSB5 site-city models. The spectral ratio drops corresponding to the certain discreet frequencies are increasing with decrease of impedance contrast between building blocks and the underlying half-space, as was observed in the case of horizontal components. However, it is interesting to note that the width of the spectral ratio drops is increasing with the decrease of IC and increase of frequency to some extent. This effect is clearly visible in the case of ICSB1 site-city model where IC is 10 and there is band gap between 3.5 to 4.0 Hz.

These spectral ratio drops for both the component of Rayleigh wave may be arising due to the signal released by the buildings which are out of phase to that of the incident Rayleigh waves. Further, the observed continuous increase of drop of spectral ratio with an increase of frequency may be due to the background scattering.

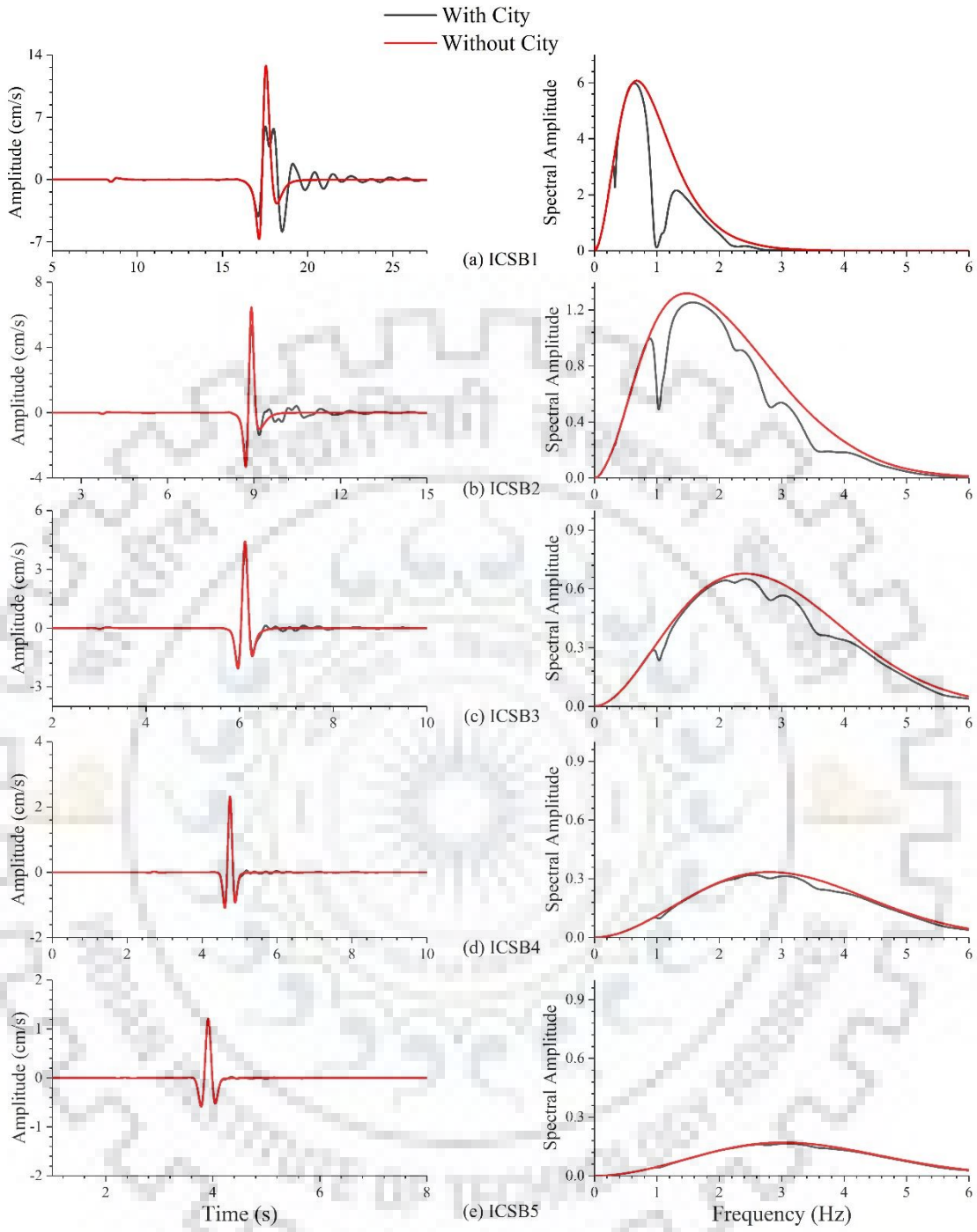


**Figure 3.6** (a) to (e) Comparison of the vertical components of the Rayleigh wave response (left panels) and spectra (right panels) at station

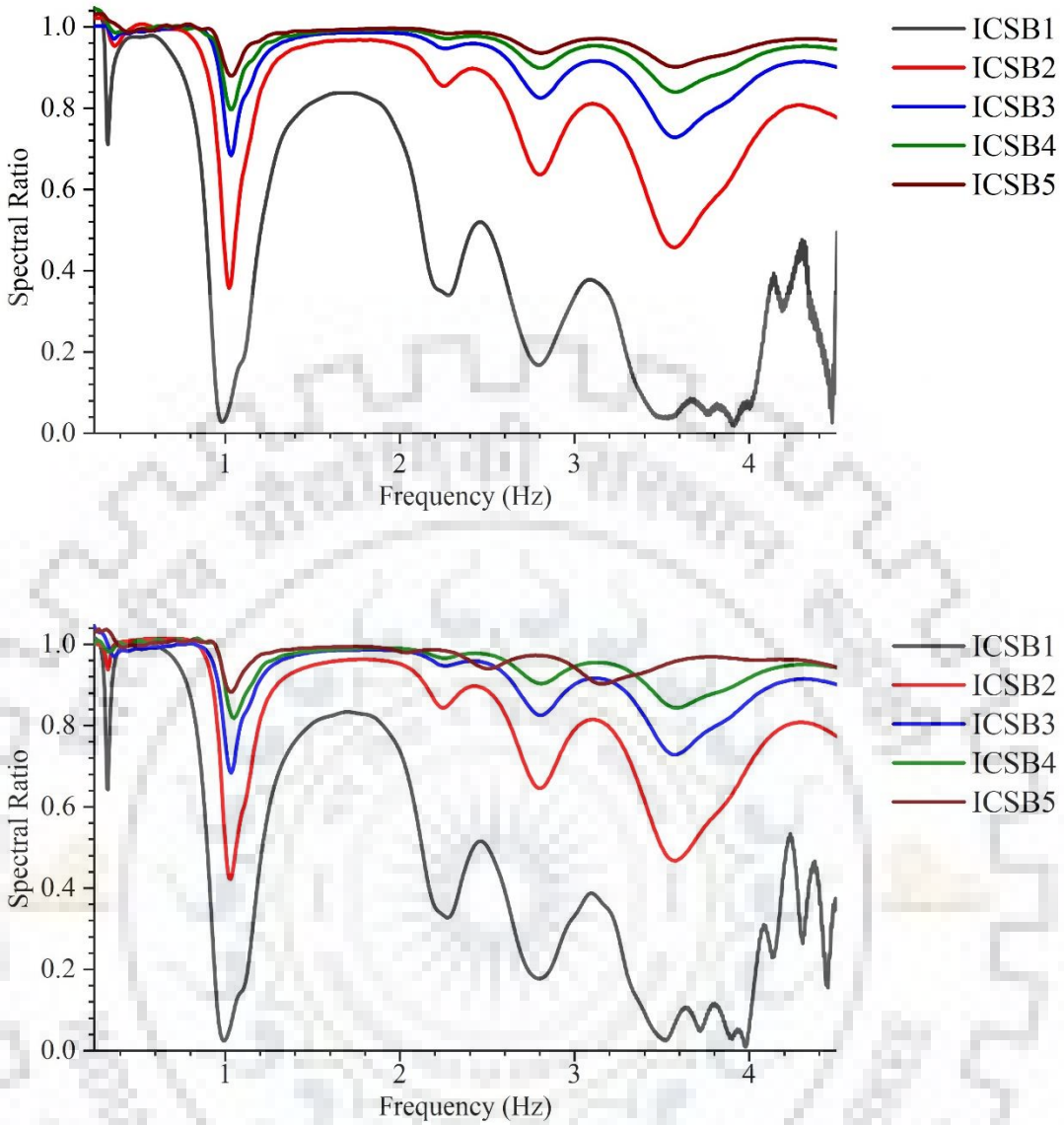


**Figure 3.7** Spectral ratio of horizontal (upper panel) and vertical (panel) component of Rayleigh wave at station

### 3.5.2 Insulating effects of city on the response of structures

In order to study the insulating effects of steel-buildings on the successive steel buildings of the city itself, the Rayleigh wave response of the model were also recorded on the top of the steel buildings. Figure 3.8 & 3.9 from (a) to (e) shows a comparison of horizontal and vertical component of the Rayleigh wave responses of the ICSB1-ICSB5 site city models on the top of S1(left panel) and S30(right panel) Steel-buildings of the city. An analysis of Figure 3.8 & 3.9 reveals a drastic decrease of amplitude of motion at the top of S30 as compared to S1 due to the insulating effects of the previous 29-steel buildings. The decrease of amplitude of Rayleigh wave at the top of both the S1 and

S30-structures with an increase of impedance in the homogeneous half-space is due to the use of a fixed stress drop in source time function (Gabor wavelet) in all the ICSB1-ICSB5. The peak particle velocity (PPV) at the top of building block in vertical components is approximately two times larger than that in horizontal component. This may be due to the larger amplitude of Rayleigh wave in the vertical component. The decrease of amplitude of motion in the horizontal and vertical component at the top of both the S1 and S30 steel-buildings with an increase of impedance in the homogeneous half-space is due to the use of a fixed stress drop in source time function (Gabor wavelet) in all the ICSB1-ICSB5 models to generate the point source.

**Table 3.7** Variation of Peak Particle Velocity at the Top S1 and S30 Steel-Buildings of the City for Different Considered Impedance Contrast Models

| Model | Horizontal Component PPV (cm/s) | | | Vertical Component PPV (cm/s) | | |
|---|---|---|---|---|---|---|
| | S1 Top | S30 Top | % Decrease | S1 Top | S30 Top | % Decrease |
| ICSB1 | 37.31 | 9.92 | 73.42 | 42.71 | 12.32 | 71.15 |
| ICSB2 | 9.45 | 3.59 | 61.90 | 28.94 | 9.29 | 67.89 |
| ICSB3 | 4.56 | 3.13 | 31.35 | 11.16 | 4.54 | 59.32 |
| ICSB4 | 2.32 | 1.74 | 25.00 | 4.65 | 2.09 | 55.00 |
| ICSB5 | 1.15 | 1.04 | 9.57 | 2.20 | 1.02 | 53.64 |

Table 3.7 shows the amplitude of motion at the top of S1 and S30 steel-buildings and the % decrease of amplitude of motion in the horizontal direction & vertical direction due to the insulating effects of building blocks. For example, the % decrease in the horizontal component at the top of S30 are 73.32%, 61.90%, 31.35%, 25.00% and 9.57% and for vertical component it is 71.15%, 67.89%, 59.32% 55.00% and 53.64% as compared to that at the top of S1 steel building for the ICSB1 to ICSB5 models, respectively. So, it can be inferred that there is drastic reduction in the response of last building of the city due to insulating effects of building blocks falling ahead and this % reduction due to insulation effect is decreasing with an increase of IC between the building blocks and the underlying half-space.

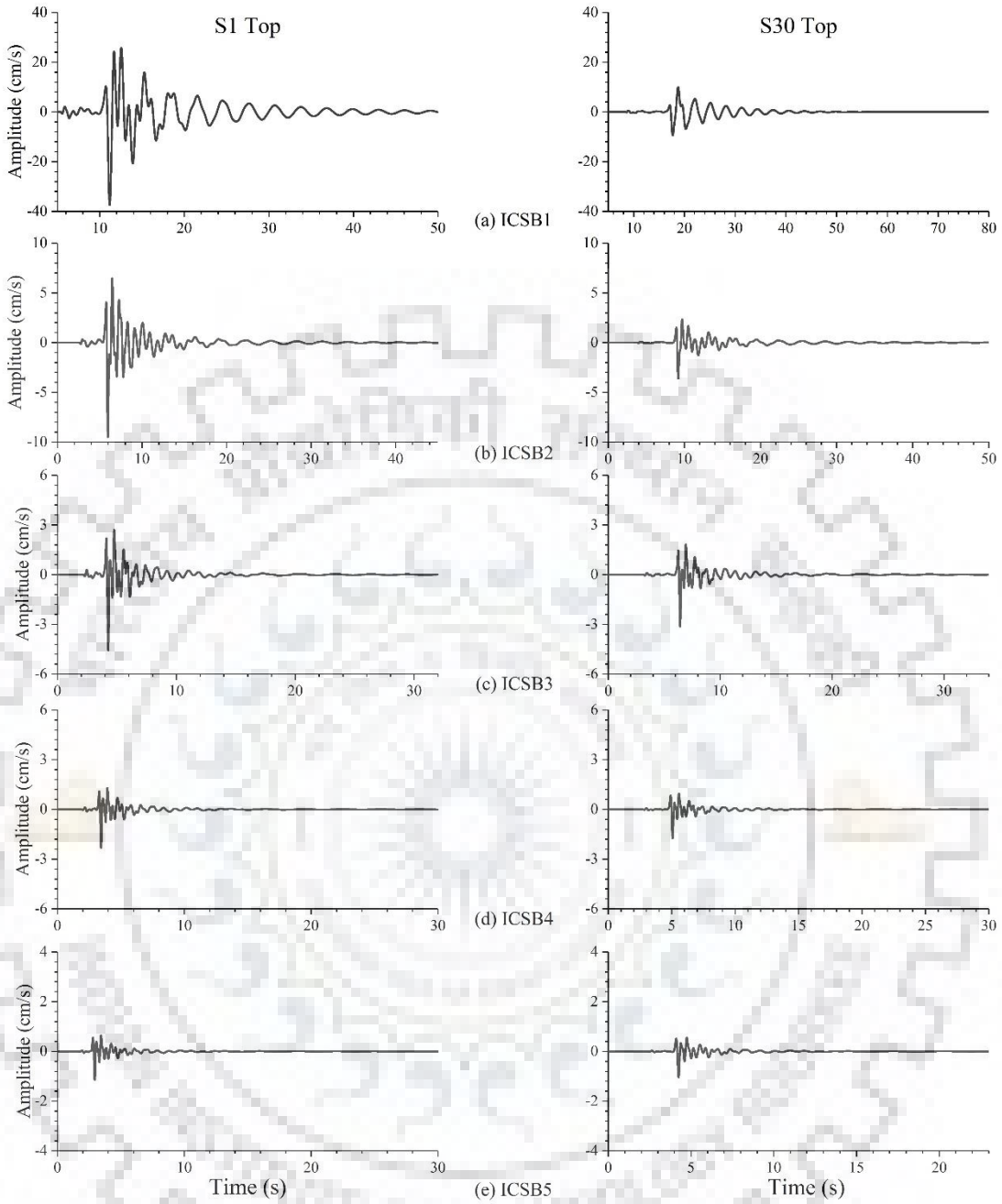


**Figure 3.8** Response of horizontal component of Rayleigh wave at the top of S1 (left panel) & S30 (right panel) steel building

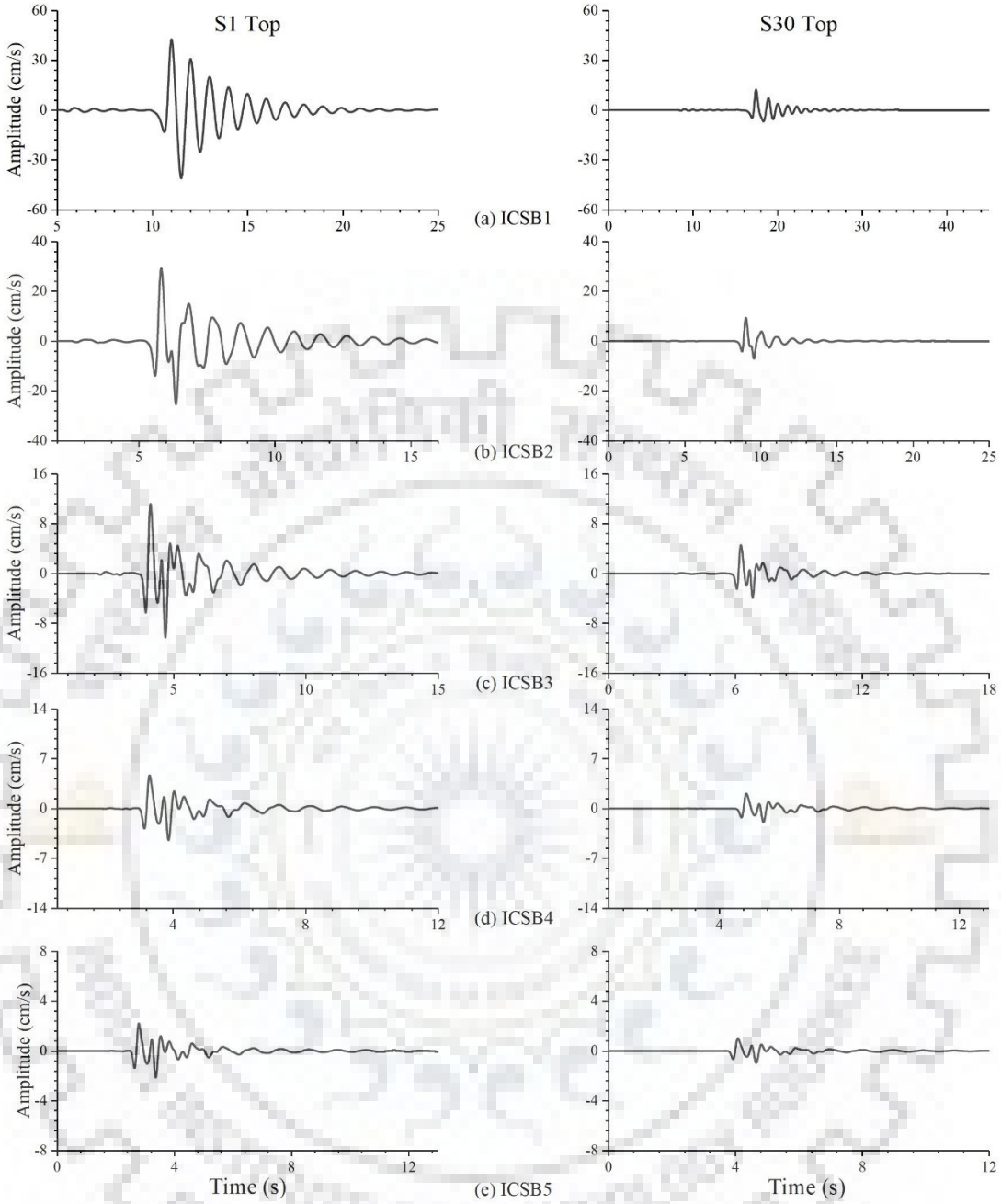


**Figure 3.9** Response of vertical component of Rayleigh wave at the top of S1 (left panel) & S30 (right panel) steel building

The left panels of Figure 3.10 (a) to (e) & Figure 3.11 (a) to (e) illustrate the comparison of spectral amplifications in the horizontal components & the vertical component at the top of S1 and S30-structures for the ICSB1 to ICSB5 site-city models, respectively. The analysis of Figure 3.10 & 3.11 depicts very large reduction in spectral amplifications at both the fundamental flexural and longitudinal modes, particularly in the case of ICSB1 model. Table 3.8 depicts the spectral amplifications at the fundamental flexural and longitudinal modes at the top of S1 and S30 structures and % reduction due to the insulating effects of steel-buildings. An analysis of Table 3.8 depicts a drastic decrease of insulation effects on the response of the S30 steel-building due to an increase of IC between building block and underlying half-space.

**Table 3.8** Comparison of Amplification at the Top S1 & S30 for Flexural and Longitudinal Modes of Vibration

| Model | Flexural modes $\left(SVF_{O2D}{}^{S}\right)$ | | | Longitudinal modes $\left(PF_{O2D}{}^{S}\right)$ | | |
|---|---|---|---|---|---|---|
| | S1 top | S30 top | %Decrease | S1 top | S30 top | %Decrease |
| ICSB1 | 33.20 | 15.72 | 52.65 | 20.04 | 3.536 | 82.35 |
| ICSB2 | 38.56 | 20.62 | 47.04 | 23.82 | 8.073 | 66.10 |
| ICSB3 | 40.68 | 30.52 | 24.97 | 24.70 | 12.10 | 51.00 |
| ICSB4 | 42.89 | 34.32 | 19.98 | 24.96 | 14.06 | 43.64 |
| ICSB5 | 43.67 | 41.58 | 4.78 | 25.68 | 16.09 | 37.32 |

The percentage decrease in spectral amplification at the top of S30 as compared to S1 building blocks is higher in fundamental longitudinal modes as compared to fundamental flexural modes and this percentage decrease in spectral amplification is decreases as the impedance contrast increase from ICSB1 to ICSB5 city models.

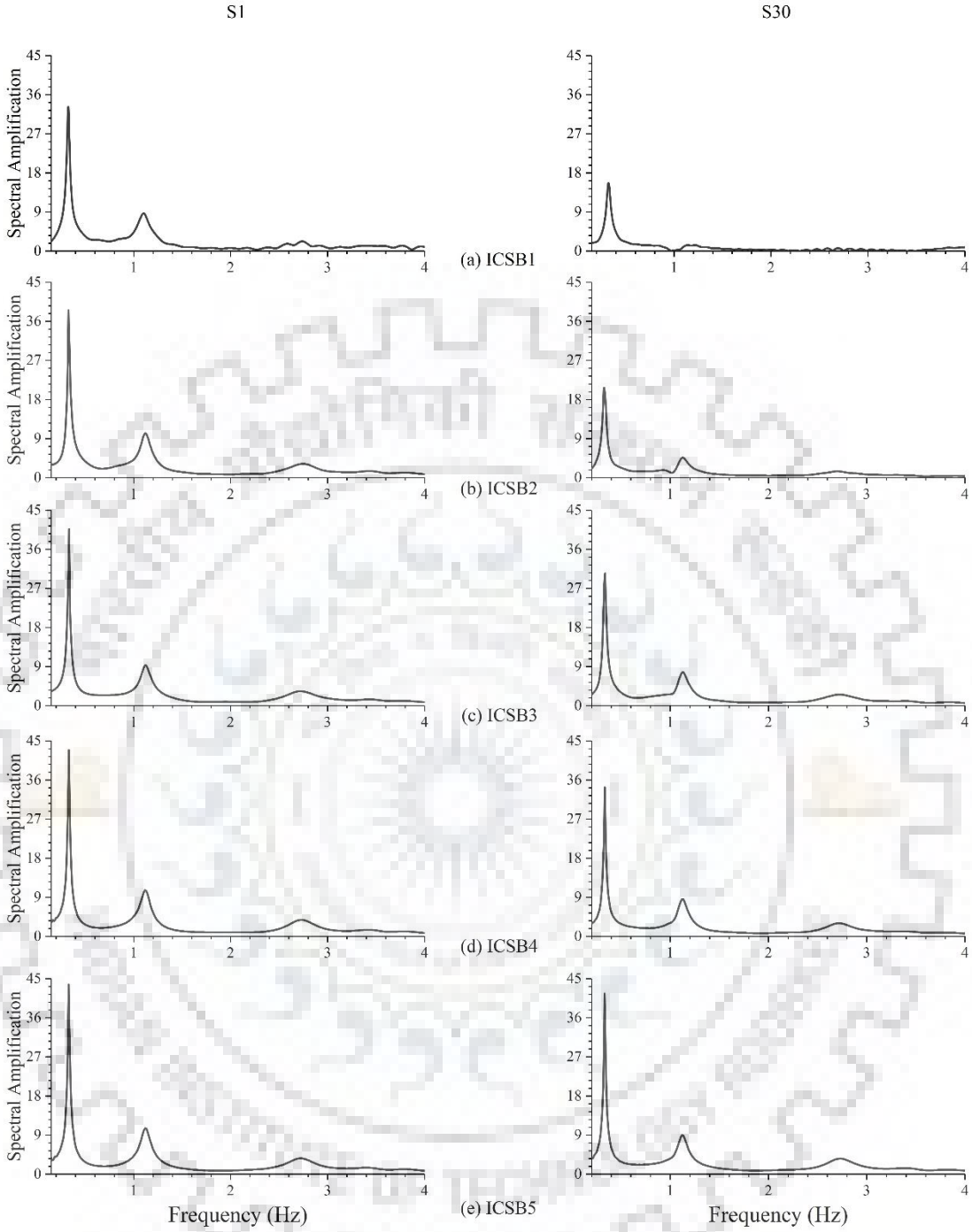


**Figure 3.10** Spectral amplification at the top of S1 (left panel) & S30 (right panel) for the horizontal component of Rayleigh wave

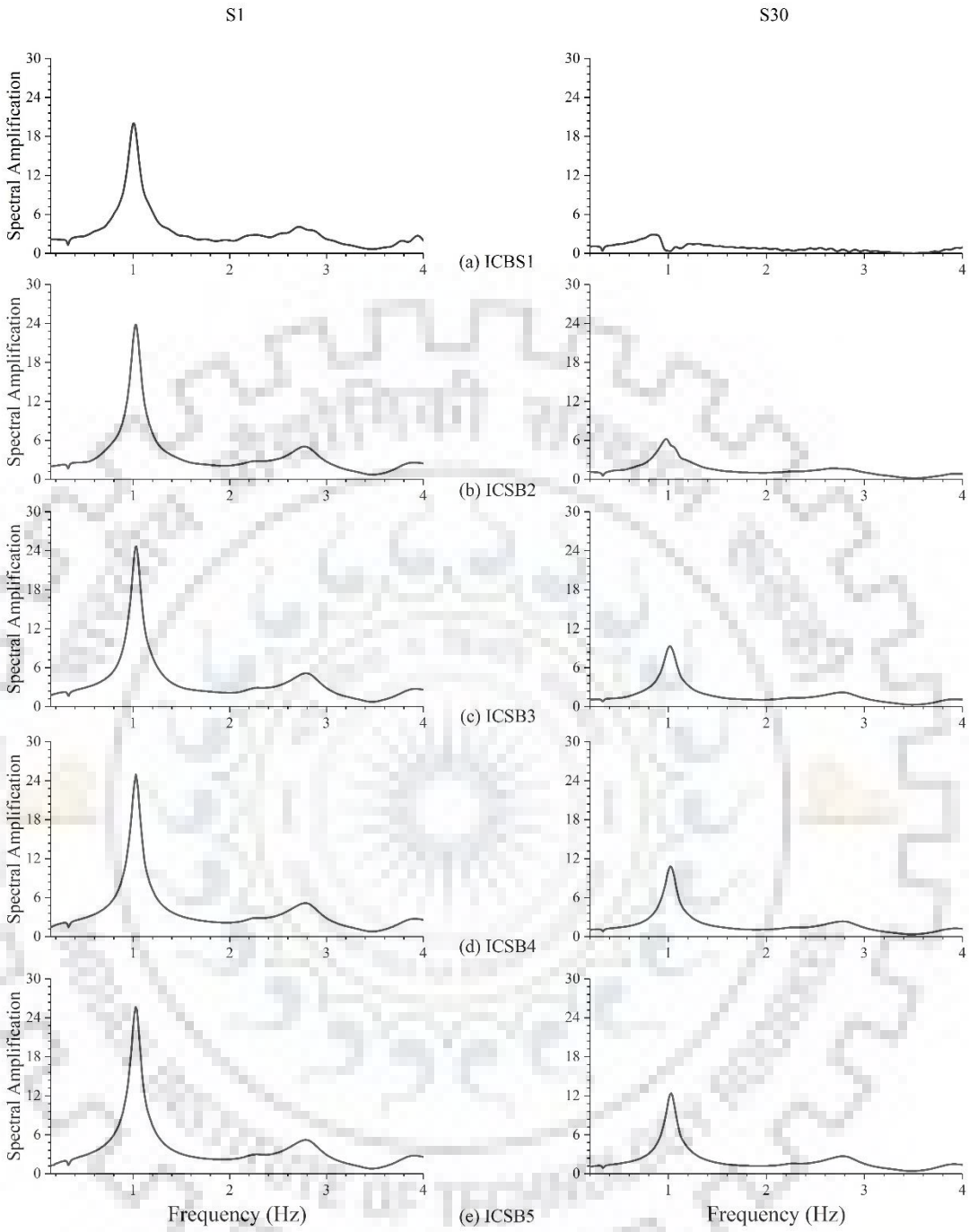


**Figure 3.11** Spectral amplification at the top of S1 (left panel) & S30 (right panel) for the vertical component of Rayleigh wave

## 3.6 Role of impedance contrast in meta-structure effect

In order to infer whether building blocks of the city (which may act as a sub-wavelength resonators) can develop a band-gap, the computed spectral ratio of responses corresponding to with and without city in the model needs further analysis. An analysis of Figure 3.7 shows the increase of spectral ratio drops at different flexural and longitudinal modes of vibrations of the steel-buildings with the decrease of IC between the building block and the underlying half-space. The spectral ratio drops at the longitudinal modes of vibrations are much larger than the flexural modes of vibrations of the building blocks. It is interesting to note that there is widening of the spectral ratio drops with the decrease of impedance contrast and the increase of modes of vibrations. In contrast to this, there is no widening of the spectral ratio drop at the fundamental flexural mode with the decrease of impedance contrast. For example, there is a band-gap of width 3.5-4.0 Hz in the case of ICSB1 model, wherein impedance contrast is 10. So, it may be inferred that there may be further increase in the spectral ratio drops and the band-gap corresponding to the different longitudinal modes of vibrations of steel-building in the cases where impedance contrast is lesser than 10. This finding corroborates with the findings of Colombi et al. (2016), wherein a development of a frequency band-gap has been reported due to the interaction of trees of a forest with the Rayleigh waves.

## 3.7 SUMMARY

The analysis of the Rayleigh wave responses of the city made-up of 30 steel buildings reveals that the buildings of the city are acting as an insulator for the Rayleigh waves. There is an increase of insulating effect with a decrease of impedance contrast between the steel buildings and the underlying half-space. The insulating effects of the steel buildings has caused around 73.42%, 61.90%, 31.35%, 25.00% and 9.5 % for horizontal component and 71.15%, 67.89%, 59.32%, 55% and 53.34% for vertical component reduction of amplitude at the top of $30^{th}$ steel building in the ICSB1 to ICSB5 site-city models, respectively. It is inferred that the building blocks may act as a meta-structure when the impedance contrast between the building blocks and the underlying half-space is less than 10 and can create a large frequency band-gaps at their different longitudinal modes of vibrations (Colombi et al., 2016).

# CHAPTER 4

# ANALYSIS OF RAYLEIGH WAVE INTERACTION WITH THE CITY MODEL MADE UP OF RC BUILDING

## 4.1 Model parameters

In this chapter, we will study the effects of interaction of Rayleigh waves with the RC buildings of the city on the characteristics of Rayleigh wave as well as on the response of building. The plan building is taken as 30m × 30 m. Building height is taken as 45m. The size of column is taken as square section of size 600mm at a spacing of 5m. The size of beam is taken as 450mm × 450 mm and live load is taken as 4 KN/m$^2$. These data is used to obtained the effective density of building blocks which is to be used in FD program instead of real building is coming out to be 600 Kg/m$^3$. The shear velocity in RC frame structure is taken as 300 m/s based on the analysis of (Clotaire & Philippe Gueguen). The fundamental frequency of RC frame structure computed using IS 1893 (Part-1):2016 is closer to the value obtained by FD simulation. For a pilot study, the considered velocity of S-Wave and P-Wave for building block and surrounding material along with the quality factor and unrelaxed moduli of rigidity is given in Table 4.1. Quality factor is inversely related to damping which is coming out to be 10 for 5% damping for RC building. The quality factor for surrounding material is taken as 10 % of the considered velocity. The inelastic parameter of building block and surrounding material corresponding to $\mu_u$, $\lambda_u$ and $K_u$ is given is given in Table 4.2.

**Table 4.1**Rahaeological Parameters of RC Building Blocks and Surrounding Material

| Material | Velocity (m/s) | | Quality Factor | | Density (kg/m$^3$) | Unrelaxed Moduli (GPa) | | |
|---|---|---|---|---|---|---|---|---|
| | $V_p$ | $V_s$ | $Q_p$ | $Q_s$ | | $\mu_u$ | $K_u$ | $\lambda_u$ |
| Block | 560 | 300 | 10 | 10 | 600 | 0.069 | 0.121 | -0.018 |
| Rock | 1720 | 700 | 172 | 700 | 1450 | 0.736 | 0.900 | -0.571 |

**Table 4.2** Inelastic Parameters of Building blocks and underlying rock

| Building Blocks | | | Rock | | |
|---|---|---|---|---|---|
| $\mu_u$ | $\lambda_u$ | $K_u$ | $\mu_u$ | $\lambda_u$ | $K_u$ |
| 0.081852777 | 0.081852777 | 0.081852777 | 0.022083598 | -0.01325117 | 0.009566398 |
| 0.090527576 | 0.090527576 | 0.090527576 | 0.019301534 | -0.01331519 | 0.008157722 |
| 0.106982582 | 0.106982582 | 0.106982582 | 0.019792335 | -0.01529167 | 0.008241645 |
| 0.174537226 | 0.174537226 | 0.174537226 | 0.024639149 | -0.02184897 | 0.010002907 |

## 4.2 Interaction of the Rayleigh wave with RC Buildings of a city: A pilot study

In order to infer the cumulative effects of interaction of Rayleigh wave with the individual RC building of the city on the response of RC itself as well as on the characteristics of the Rayleigh wave after crossing the city, the seismic response of a city made up of 30 RC buildings with length/width and height 30m and 45m respectively, computed at the top of the buildings and at the free surface at an epicentral distance of 3300m. Model parameters used for this study is given in Table 4.1.

### 4.2.1 Response of RC Buildings

Figure 4.1(a) depicts a comparison of horizontal (left panel) and vertical (right panel) components of response of S1-building with the free field motion at the same location. In both the horizontal and vertical component, there is drastic increase of duration of motion and amplitude at the top of S1-building as compared to the free field motion at that location.

The left and right panels of Figure 4.1 (b) shows the comparison of spectral of the horizontal (left panel) and vertical components (right panel) of response of S1 RC building with the free field motion. An analysis of Figure 4.1 (b) depicts spectral peaks at discrete frequencies in both the components. These simulated fundamental flexural ($SVF^{S}_{O2D}$) and longitudinal ($PF^{S}_{O2D}$) modes of vibration for the SV-wave and P-wave matches with the empirically computed using equations given by Kumar and Narayan (2018).

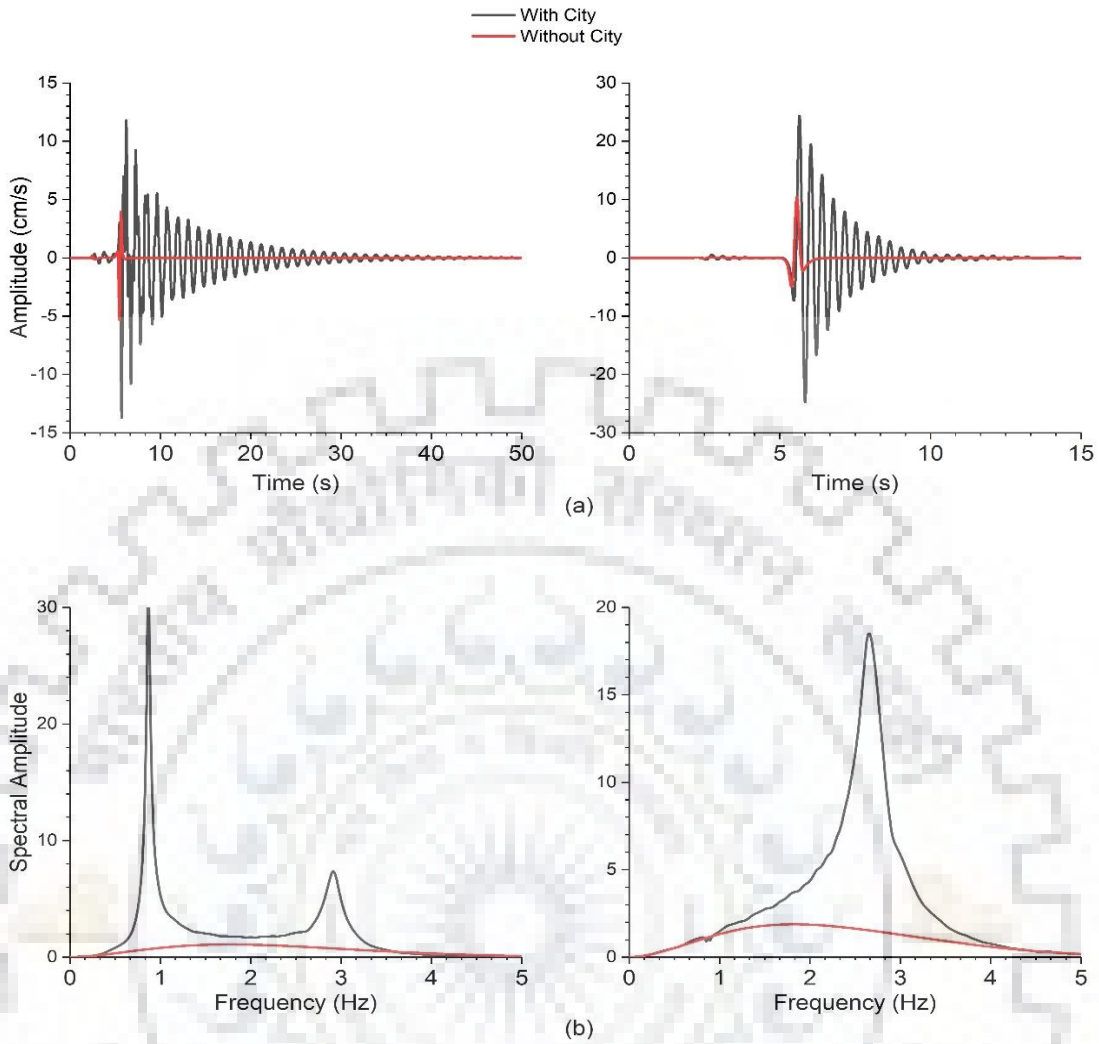


s

**Figure 4.1** (a) Comparison of horizontal (left panel) and vertical (right panel) components of response at the top of S1 building and free filed motion (b) comparison of spectra of horizontal (left panel) and vertical (right panel) components of responses at the top of S1 building and free field motion

**Table 4.3** Comparison of Computed & Simulated Fundamental Flexural and Longitudinal Frequency of the Building Block

| S.No. | Component | FD Simulation | Empirical relation |
|---|---|---|---|
| 1 | $SVF^{S}_{02D}$ | 0.86 Hz | 0.81 Hz |
| 2 | $PF^{S}_{02D}$ | 2.76 Hz | 2.81 Hz |

### 4.2.2 Response at the free field recorder

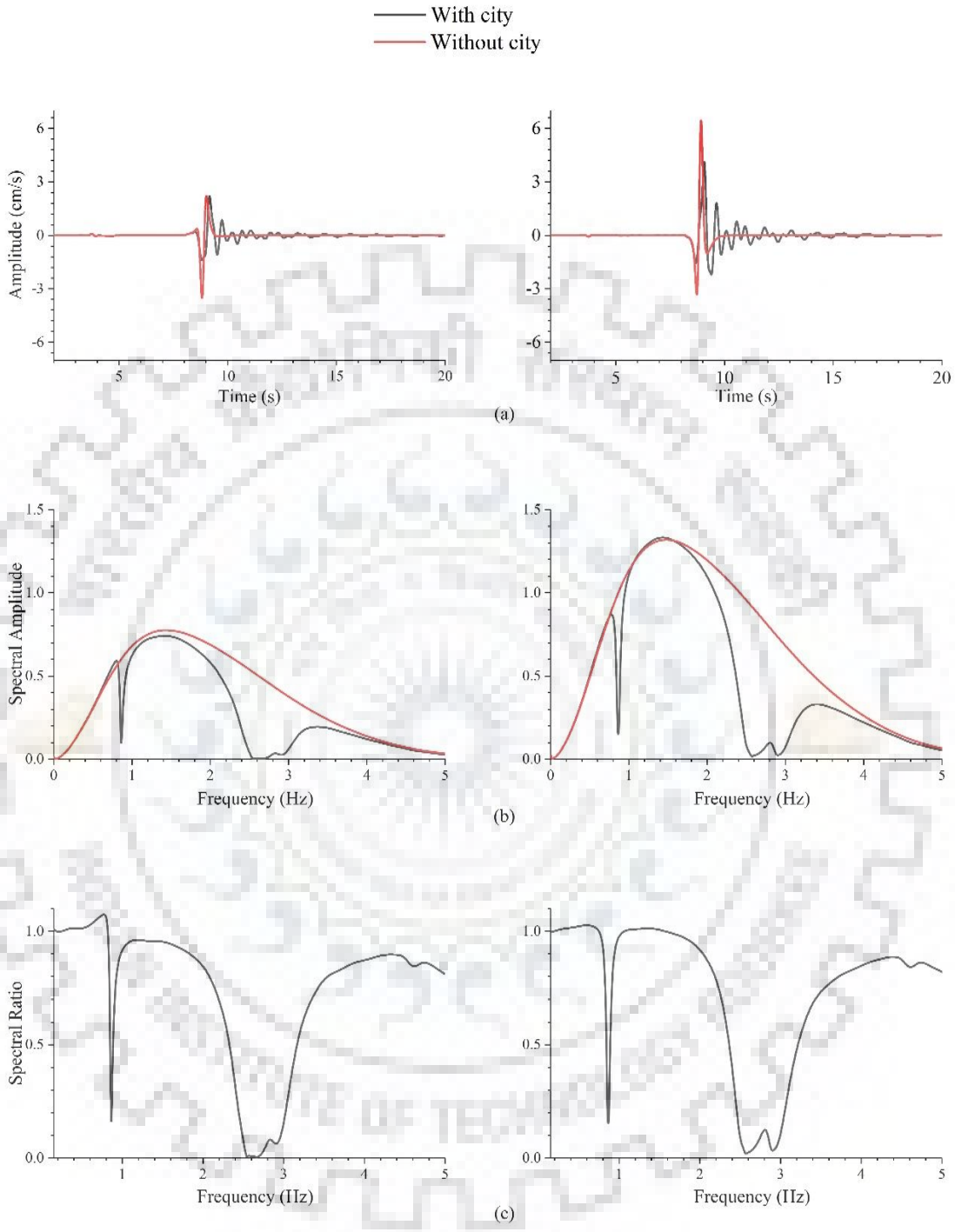


**Figure 4.2** (a) Comparison of response of Rayleigh wave at station (b) a comparison of spectra (c) spectral ratios for the horizontal and vertical components of Rayleigh wave at the recording station

The left and right panels of Figure 4.2(a) show the comparison of horizontal and vertical component of the response of the site-city model at the recording station with that in the absence of the city. A decrease of the Rayleigh wave amplitude after crossing

the city can be inferred. There is around 32% and 36% decrease of amplitude of Rayleigh wave in the horizontal and vertical components after interacting with the 30 RC building blocks of the city. There is an increase of duration of ground motion in the case of response of the city. These extra phases may be due to the vibrations of the individual RC buildings of the city. The vibrating structures may release their energy to the earth in the form of body and the surface waves. Similarly, the left and right panels of Figure 4.2(b) show the comparison of spectra of the horizontal and vertical components of the response of the site-city model at the recording station with those in the absence of city. An analysis of Figure 4.2(b) shows drops in the spectra corresponding to the different modes of the flexural and longitudinal vibrations of the building blocks. These drops may be arising due to the phase difference (out of phase) of $\pi$ between the waves released by the building blocks as compared to the free field ground motion in the absence of city.

The left and right panels of Figure 4.2(c) show the spectral ratio of the horizontal and vertical components of the free field motion corresponding to with and without city in the model. An analysis of Figure 4.2(c) shows spectral ratio drops corresponding to the different modes of flexural and longitudinal vibrations of the building blocks Value of spectral ratio drop corresponding to the fundamental longitudinal mode of vibration of building blocks is the largest one. On the other hand, the value of spectral ratio drop corresponding to the flexural fundamental mode of vibration of building blocks is less as compared to the fundamental longitudinal mode of vibration. Further, considerable spectral ratio drops corresponding to the higher longitudinal modes of vibrations of the building block can be inferred in both the components of the Rayleigh wave. It is interesting to note that the observed different spectral ratio drops are same in both the components of the Rayleigh wave.

Figure 4.2(c) also reveals a continuous decrease in the spectral amplitude of Rayleigh in both the horizontal and vertical components of Rayleigh wave with the increasing frequency. This may be due to the background scattering of the Rayleigh wave during the interaction of the RC-buildings. From the above result, it is inferred that the RC buildings of city are acting as an insulator for the Rayleigh wave as well as a sub-wavelength resonator.

## 4.3 Role of Impedance contrast in Insulating Effect of RC Buildings

### 4.3.1 Insulating effects on free field motion

To study the role of impedance contrast between the building blocks and the underlying earth material in the insulating effects of buildings on the characteristics of the Rayleigh wave, the Rayleigh wave responses of the various site-city models with the same source parameters as well as the numbers on buildings and the rheological parameters of the building blocks but with a varying impedance in the homogeneous half-space were computed and analyzed. For this study, five-different impedance contrast models namely ICRC1, ICRC2, ICRC3, ICRC4 and ICRC5 with different impedance in homogeneous half-space rock are taken whose rheological parameters are given in the Table 4.4 and inelastic parameters of different impedance of underlying homogeneous surrounding materials are given in Table 4.5.

**Table 4.4** Rheological Parameter of the Half-Space in the ICRC1-ICRC5 Impedance Contrast Models (Rheological Parameters of Building Blocks are same as given in Table 4.1)

| IC models | Velocity (m/s) | | Quality factor (Q) | | Density ($kg/m^3$) | IC for S-wave | Unrelaxed moduli (GPa) | | |
|---|---|---|---|---|---|---|---|---|---|
| | $V_P$ | $V_S$ | $Q_P$ | $Q_S$ | | | $\mu_u$ | $K_u$ | $\lambda_u$ |
| ICRC1 | 700 | 350 | 70 | 35 | 1200 | 2.33 | 0.157 | 0.152 | -0.163 |
| ICRC2 | 1720 | 700 | 172 | 70 | 1450 | 5.64 | 0.735 | 0.900 | -0.571 |
| ICRC3 | 2200 | 1050 | 220 | 105 | 1700 | 9.92 | 1.918 | 1.467 | -2.365 |
| ICRC4 | 2615 | 1400 | 262 | 140 | 1950 | 15.17 | 3.889 | 2.070 | -5.707 |
| ICRC5 | 3100 | 1750 | 310 | 175 | 2200 | 21.39 | 6.832 | 2.905 | -10.758 |

**Table 4.5** Inelastic parameters of different impedance underlying homogeneous models.

| Model | $\mu_u$ | $\lambda_u$ | $K_u$ |
|---|---|---|---|
| ICRC1 | 0.03974669 | -0.0101144 | 0.022083598 |
| | 0.036188727 | -0.01323824 | 0.019301534 |
| | 0.038044929 | -0.01739541 | 0.019792335 |
| | 0.049455655 | -0.02936735 | 0.024639149 |
| ICRC2 | 0.022083598 | -0.01325117 | 0.009566398 |
| | 0.019301534 | -0.01331519 | 0.008157722 |
| | 0.019792335 | -0.01529167 | 0.008241645 |
| | 0.024639149 | -0.02184897 | 0.010002907 |
| ICRC3 | 0.015248292 | -0.00648502 | 0.007549355 |
| | 0.013144519 | -0.00655553 | 0.006413811 |
| | 0.013366622 | -0.00759527 | 0.006465348 |
| | 0.016403894 | -0.0108688 | 0.007817404 |
| ICRC4 | 0.011638556 | -0.0034632 | 0.006396973 |
| | 0.009963394 | 0.000895159 | 0.006865145 |
| | 0.010089443 | -0.00131428 | 0.006335002 |
| | 0.012294237 | -0.00179562 | 0.00785821 |
| ICRC5 | 0.009409305 | -0.00188061 | 0.005409897 |
| | 0.008021421 | -0.00205596 | 0.004578389 |
| | 0.00810252 | -0.00252244 | 0.004604471 |
| | 0.00983113 | -0.00378087 | 0.005545549 |

**Table 4.6** Peak Ground velocity (PGV) at the Recording Station in the Presence And Absence of the City for Both the Components of the Rayleigh Waves

| Model | Horizontal component (PGV)(cm/s) | | | Vertical component (PGV)(cm/s) | | |
|---|---|---|---|---|---|---|
| | With city | Without city | % Decrease | With city | Without city | % Decrease |
| ICRC1 | 4.75 | 7.68 | 38.00 | 7.65 | 12.77 | 40.09 |
| ICRC2 | 2.20 | 3.51 | 37.32 | 3.98 | 6.44 | 38.20 |
| ICRC3 | 1.46 | 2.27 | 35.68 | 2.84 | 4.42 | 35.74 |
| ICRC4 | 0.88 | 1.23 | 28.46 | 1.58 | 2.32 | 31.89 |
| ICRC5 | 0.53 | 0.66 | 19.96 | 0.95 | 1.21 | 21.48 |

The left panels of Figure 4.3 & 4.4 from (a) to (e) show a comparison of the horizontal and vertical component of the Rayleigh wave responses of the ICRC1 to ICRC5 site-city models corresponding to with and without city in the model at the recording station. Similarly, the right panels of figure 4.3 & 4.4 from (a) to (e) show a comparison of spectra of the horizontal component of the Rayleigh wave responses of the ICRC1 to ICRC5 site-city models corresponding to with and without city in the model at the recording station. The decrease of amplitude of Rayleigh wave and corresponding spectra in both the responses (with and without the city in the model) with an increase of impedance in the homogeneous half-space is due to the use of a fixed stress drop in source time function (Gabor wavelet) in all the ICRC1 to ICRC5 site-city models to generate the point source.

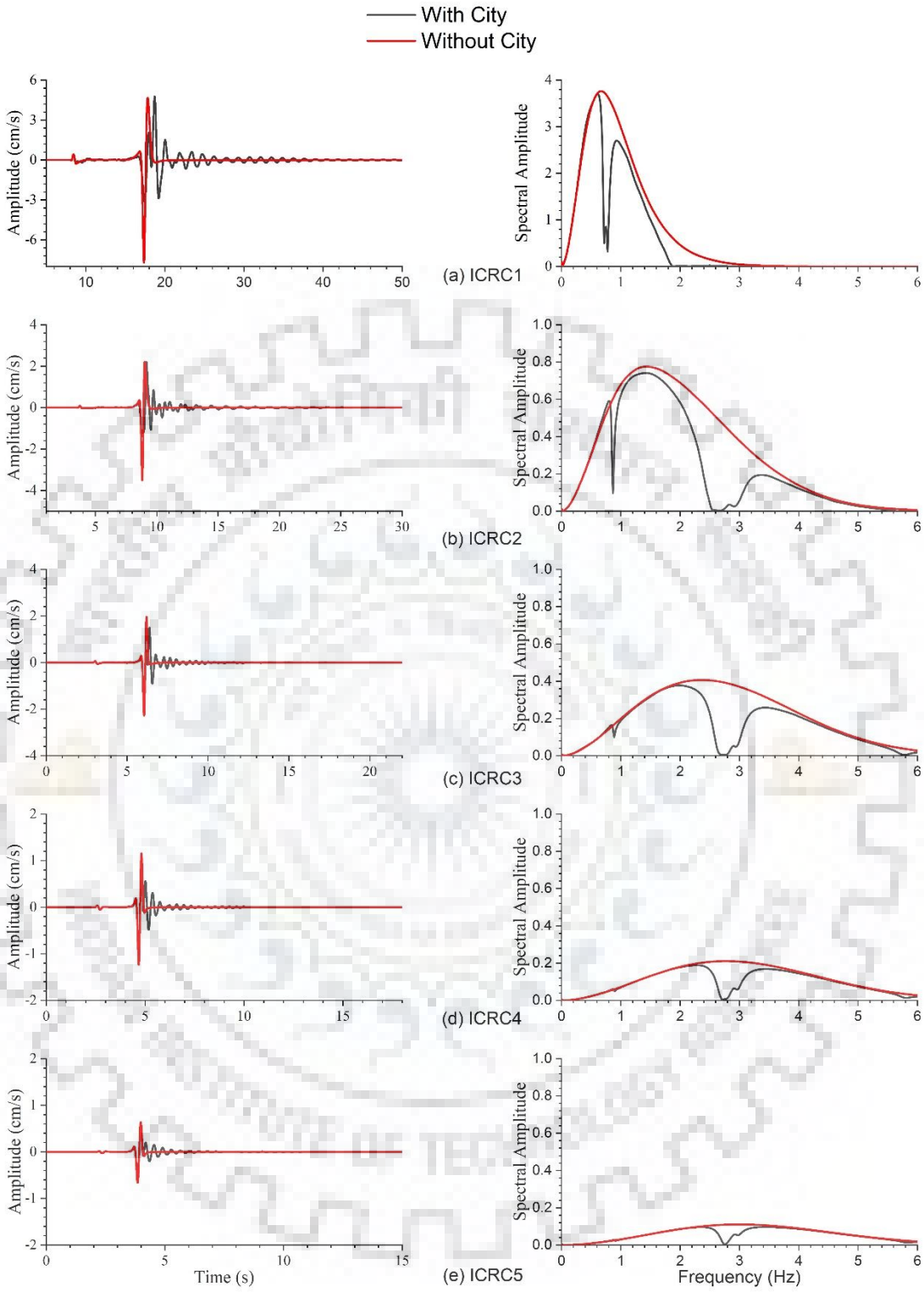


**Figure 4.3** (a) to (e) Comparison of the horizontal components of the Rayleigh wave response (left panels) and spectra (right panels) at recording station

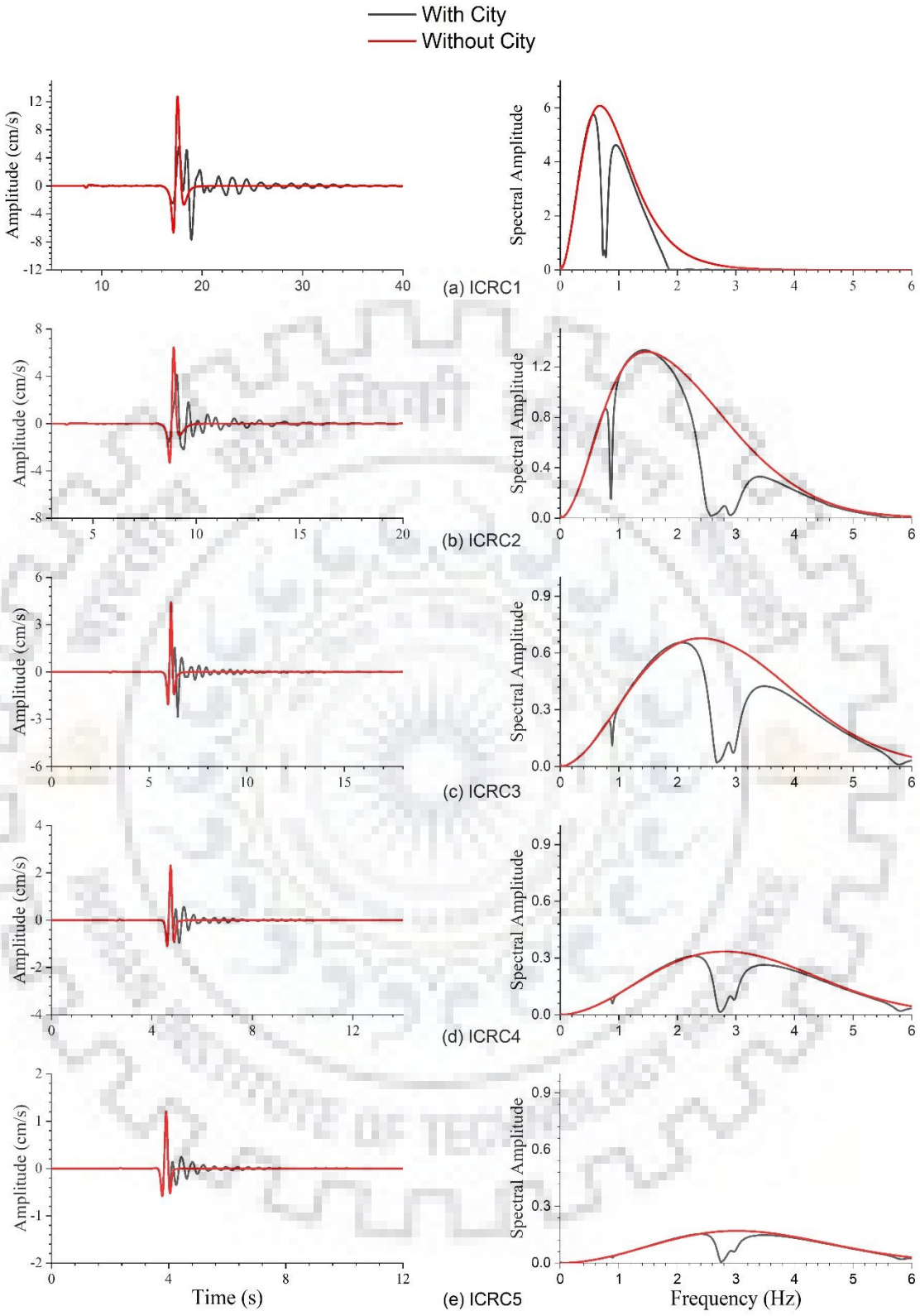


**Figure 4.4** (a) to (e) Comparison of the vertical components of the Rayleigh wave response (left panels) and spectra (right panels) at recording station

The analysis of both the Figure 4.3 & 4.4 reveals that as the impedance contrast between the RC-buildings and the underlying half-space is decreasing, the amplitude decrease due to the insulating effects of RC-buildings is increasing. Table 4.6 shows the amplitude of Rayleigh wave (both horizontal & vertical component) corresponding to without and with city in the model and the % decrease of amplitude of the Rayleigh waves due to the insulating effects of RC-buildings. For example, the % amplitude decrease of the Rayleigh wave in the horizontal component are 38%, 37.32%, 35.68%, 28.46% and 19.69% and 40.09%, 38.20%, 35.74%,31.89% and 21.48% for the vertical component in the ICRC1 to ICRC5 site-city models. Further, there is an increase of value of drops in the spectra of Rayleigh wave corresponding to different modes of flexural and longitudinal vibrations of the RC-buildings with the decrease of impedance contrast. So, it can be inferred that there is an increase of insulating effects of the RC-buildings with a decrease of impedance contrast between the building blocks and the underlying half-space.

Figure 4.5 show the spectral ratio drops at the discreet fundamental flexural and longitudinal frequency for horizontal component (upper panel) & vertical component (lower panel) of Rayleigh wave corresponding to ICRC1 to ICRC5 site city model. Analysis of Figure 4.5 shows the spectral ratio drops corresponding to the certain discreet frequencies are increasing with decrease of impedance contrast between building blocks and the underlying half-space. However, there is no change of frequency corresponding to these spectral ratio drops with decrease of IC. But it is interesting to note that the width of the spectral ratio drops is increasing with the decrease of IC and increase of frequency to some extent. This effect is clearly visible in the case of ICRC1 site-city model where IC is 2.33 and there is band gap between 1.8 to 3.2 Hz.

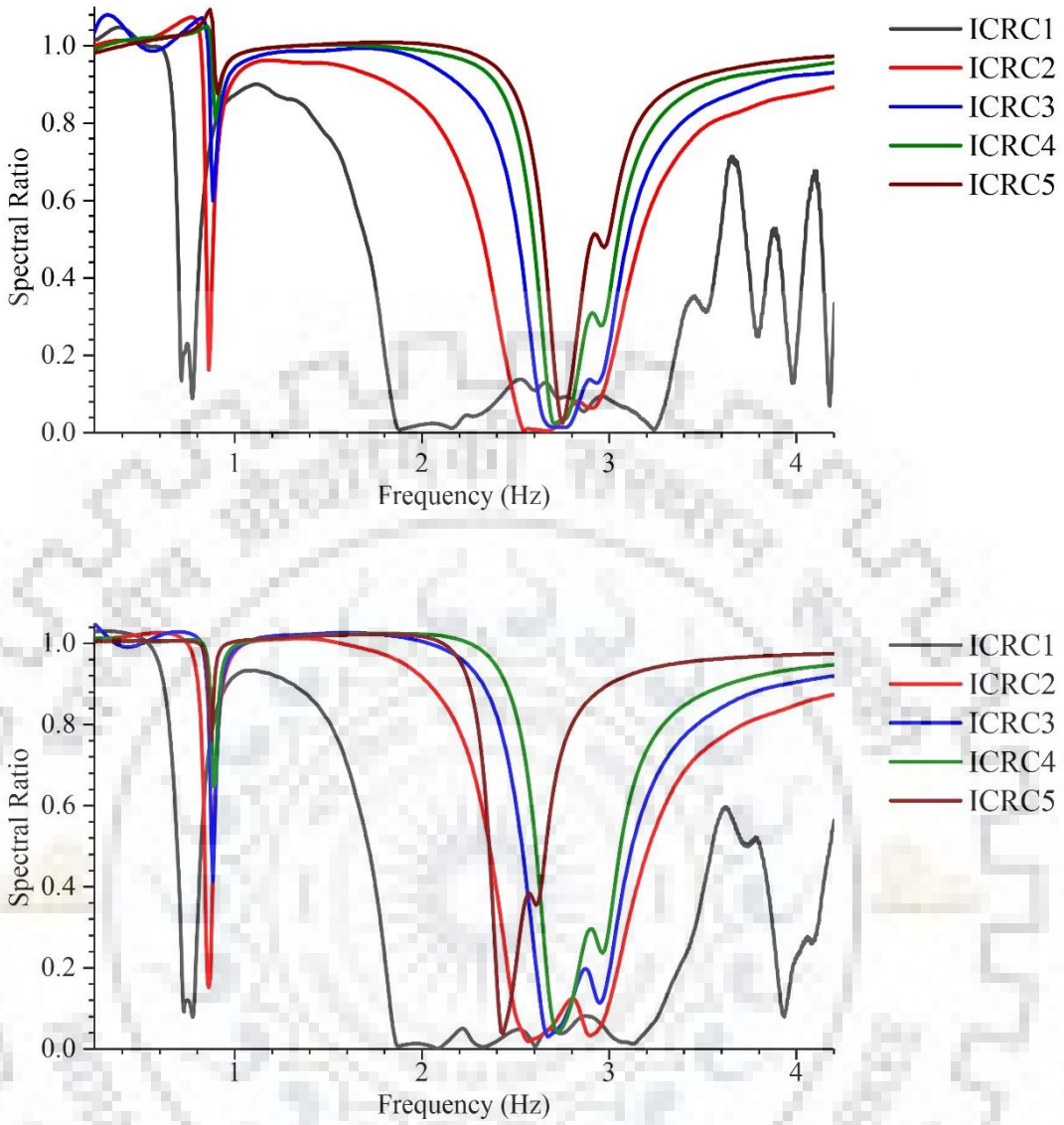


**Figure 4.5** Comparison of spectral ratio for horizontal (upper panel) and vertical (lower panel) component of Rayleigh wave

### 4.3.2 Insulating effects of city on the response of structures

In order to study the insulating effects of RC buildings on the successive RC-buildings of the city itself, the Rayleigh wave response of the model were also recorded on the top of the RC-buildings. Figure 4.6 & 4.7 from (a) to (e) shows a comparison of horizontal and vertical component of the Rayleigh wave responses of the ICRC1-ICRC5 site city models on the top of S1(left panel) and S30(right panel) RC-buildings of the city. An analysis of figure 4.6 & 4.7 reveals a drastic decrease of amplitude of motion at the top of S30 as compared to S1 due to the insulating effects of the previous 29-RC buildings. of a fixed stress drop in source time function (Gabor wavelet) in all the ICRC1 to ICRC5. The peak particle velocity at the top of building block in vertical components is approximately two times larger than that in horizontal component. This may be due to the larger amplitude of Rayleigh wave in the vertical component. The decrease of amplitude of motion in the horizontal and vertical component at the top of both the S1 and S30 RC-buildings with an increase of impedance in the homogeneous half-space is due to the use of a fixed stress drop in source time function (Gabor wavelet) in all the ICRC1 to ICRC5 models to generate the point source. Peak particle velocity at the top of S1 and S30 RC building blocks along with the percentage decrease due to 29 RC building is given in Table 4.7.

**Table 4.7** Variation of peak particle velocity at the top S1 and S30 RC-buildings city for different considered impedance contrast models

| Model | Horizontal Component PPV (cm/s) | | | Vertical Component PPV (cm/s) | | |
|---|---|---|---|---|---|---|
| | S1 Top | S30 Top | % Decrease | S1 Top | S30 Top | % Decrease |
| ICRC1 | 31.93 | 9.09 | 71.53 | 12.43 | 5.94 | 52.44 |
| ICRC2 | 7.62 | 3.55 | 53.41 | 8.24 | 4.44 | 46.48 |
| ICRC3 | 3.10 | 1.54 | 50.32 | 6.20 | 4.07 | 34.35 |
| ICRC4 | 1.43 | 0.92 | 35.67 | 2.76 | 2.25 | 18.62 |
| ICRC5 | 0.67 | 0.53 | 20.89 | 1.62 | 1.43 | 11.72 |

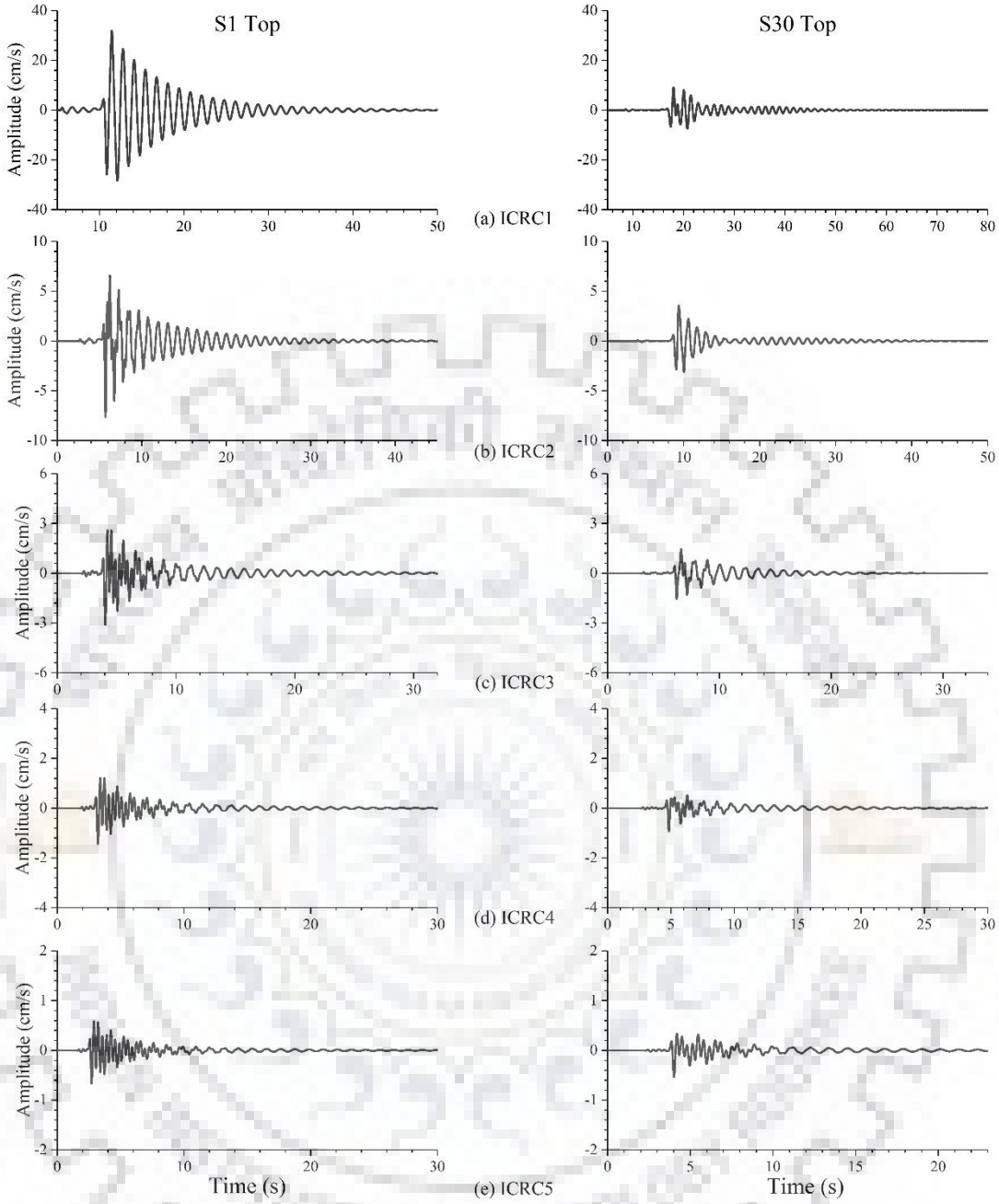


**Figure 4.6** Response of horizontal component of Rayleigh wave at the top of S1 (left panel) & S30 (right panel) RC building

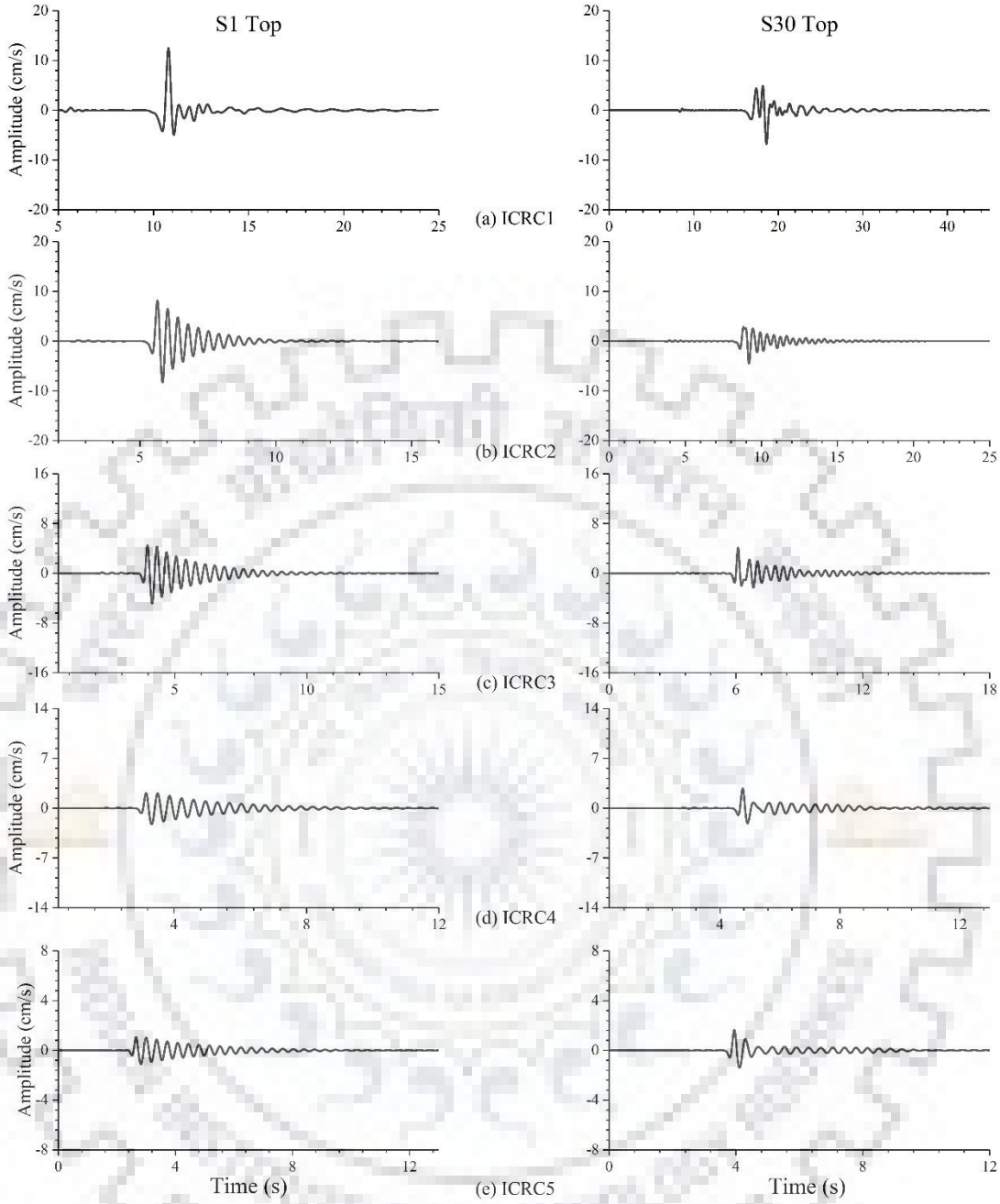


**Figure 4.7** Response of vertical component of Rayleigh wave at the top of S1 (left panel) & S30 (right panel) RC building

Table 4.7 shows the amplitude of motion at the top of S1 and S30 RC-buildings and the % decrease of amplitude of motion in the horizontal direction & vertical direction due to the insulating effects of building blocks. For example, the % decrease in the horizontal component at the top of S30 are 67.48%, 53.25%, 50.26%, 36.04% and 24.37% and for vertical component it is 72.98%, 72.85%, 57.58% 38.79% and 26.42% as compared to that at the top of S1 RC building for the ICRC1 to ICRC5 models, respectively. So, it can be inferred that there is drastic reduction in the response of last building of the city due to insulating effects of building blocks falling ahead and this % reduction due to insulation effect is decreasing with an increase of IC between the building blocks and the underlying half-space. Percentage reduction in the amplitude at the top of S30 as compared to the top of S1 is higher in case of vertical component of Rayleigh wave as compared to the horizontal component of Rayleigh wave.

The left panels of Figure 4.8(a) to (e) and Figure 4.9 (a) to (e) illustrate the comparison of spectral amplifications in the horizontal components & the vertical component at the top of S1 and S30-structures for the ICRC1 to ICRC5 site-city models, respectively. The analysis of Figure 4.8 and 4.9 depicts very large reduction in spectral amplifications at both the fundamental flexural and longitudinal modes of vibration, particularly in the case of ICRC1 model. Table 4.8 depicts the spectral amplifications at the fundamental flexural and longitudinal modes at the top of S1 and S30 structures and % reduction due to the insulating effects of 29 RC-buildings blocks falling in the path of Rayleigh wave. An analysis of Table 4.8 depicts a drastic decrease of insulation effects on the response of the S30 RC-building blocks as compared to S1 building blocks due to an increase of IC between building block and underlying homogeneous half-space.

**Table 4.8** Comparison of amplification at the top S1 & S30 for flexural and longitudinal modes of vibration and % decrease in in amplification

| Model | Flexural modes | | | Longitudinal modes | | |
|---|---|---|---|---|---|---|
| | S1 top | S30 top | %Decrease | S1 top | S30 top | % Decrease |
| ICRC1 | 20.79 | 6.31 | 69.64 | 0.82 | 0.06 | 91.46 |
| ICRC2 | 25.27 | 10.80 | 57.26 | 4.61 | 0.45 | 90.24 |
| ICRC3 | 25.42 | 16.19 | 36.31 | 7.17 | 1.14 | 84.11 |
| ICRC4 | 26.07 | 19.64 | 24.66 | 8.48 | 1.97 | 76.77 |
| ICRC5 | 26.52 | 23.11 | 12.86 | 9.33 | 2.91 | 68.81 |

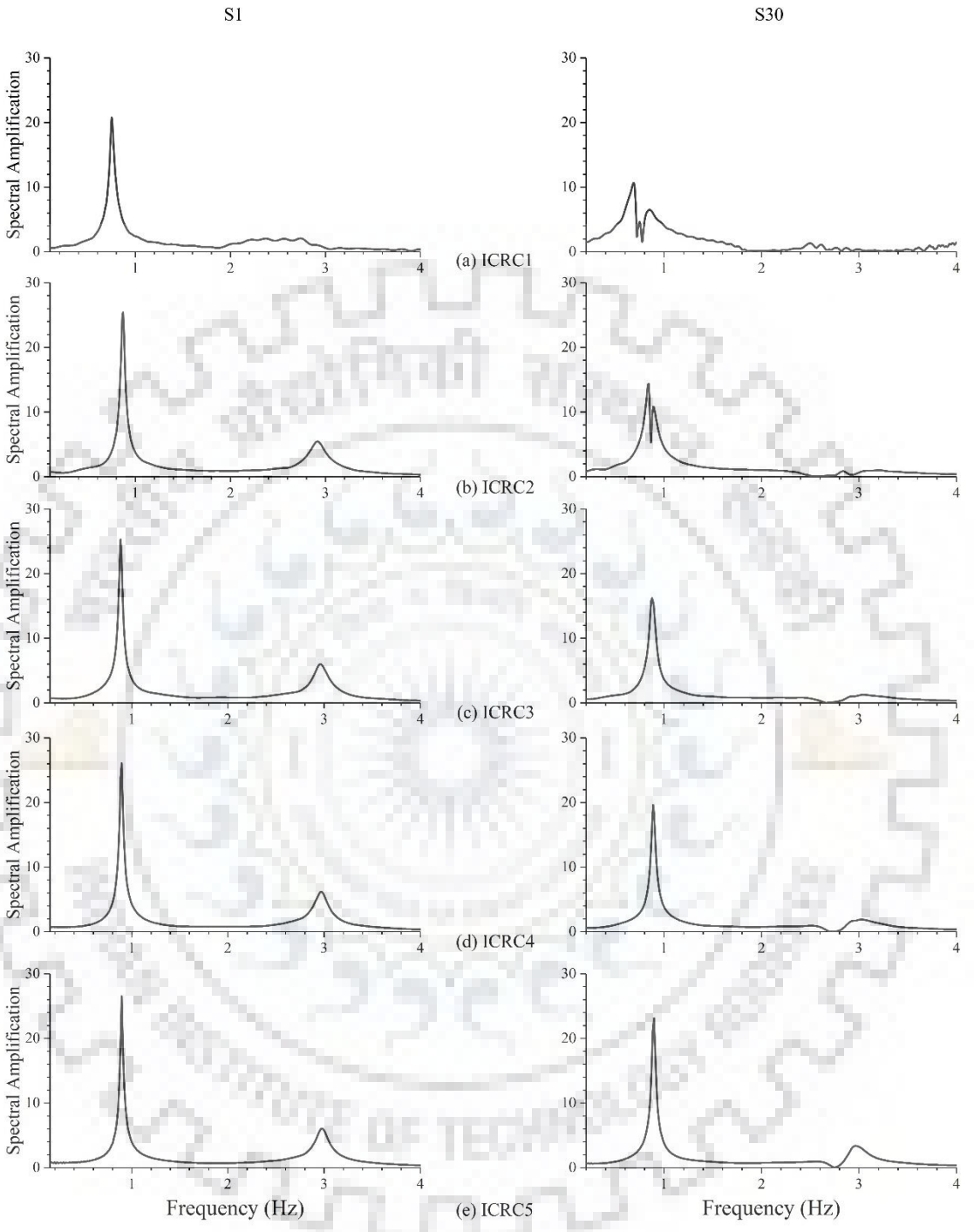


**Figure 4.8** Spectral amplification at the top of S1 (left panel) & S30 (right panel) for the horizontal component of Rayleigh wave

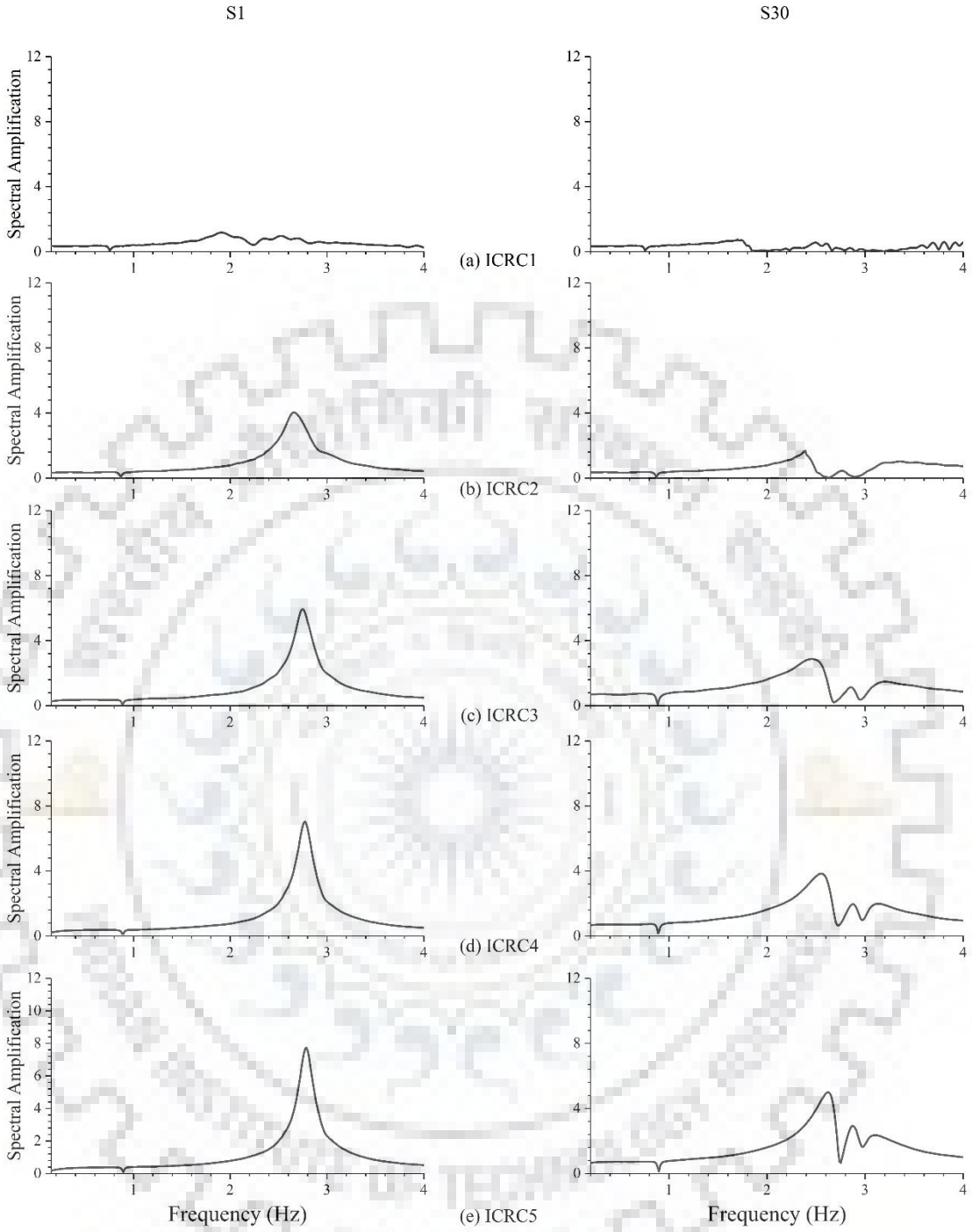


**Figure 4.9** Spectral amplification at the top of S1 (left panel) & S30 (right panel) for the vertical component of Rayleigh wave

### 4.3.3 Insulating Effect of RC building when IC=1

From the previous analysis of both the Chapter 3 and 4 we observe that as the impedance contrast between the building blocks and underlying homogeneous rock decreases, the width of spectral ratio increases, as insulating effect of building blocks increases and maximum width observe corresponding to the lowest impedance contrast to further study what will happen when impedance contrast between the building blocks and surrounding rock equal to approximately one. For this study, the velocity of P-wave, SV-wave and density so chosen that its impedance is equal to the ICRC1 to obtain impedance contrast equal to one which is obtained by taking the ratio of impedance of surrounding rock and building block.

The parameters of building blocks are given in Table 4.9 and its corresponding inelastic parameters are given in Table 4.10 (parameters of rocks and its inelastic parameters are same as that for ICRC1 model).

**Table 4.9** Parameters of Building Blocks (Parameters of Rock are same as that ICRC1 model)

| Material | Velocity (m/s) | | Quality Factor | | Density (kg/m$^3$) | Unrelaxed Moduli (GPa) | | |
|---|---|---|---|---|---|---|---|---|
| | $V_P$ | $V_s$ | $Q_P$ | $Q_S$ | | $\mu_u$ | $K_u$ | $\lambda_u$ |
| Blocks | 800 | 450 | 10 | 10 | 920 | 0.756 | 0.240 | -1.272 |

**Table 4.10** Inelastic Parameters of Building Blocks (Parameters of Surrounding Rocks are same as for ICRC1 Model)

| Model | $\mu_u$ | $\lambda_u$ | $K_u$ |
|---|---|---|---|
| Building blocks | 0.022083598 | 0.07194469 | 0.03974669 |
| | 0.019301534 | 0.068728503 | 0.036188727 |
| | 0.019792335 | 0.075232674 | 0.038044929 |
| | 0.02463914 | 0.103462154 | 0.049455655 |

In order to infer the characteristics of Rayleigh wave at the recording station after crossing the city having 30 equally spaced RC building each having same width and height, response of Rayleigh wave is recorded at the recording station in the presence and absence of city which is shown in Figure 4.10.

Figure 4.10(a) shows the response of Rayleigh wave at the recording station for both horizontal (left panel) and vertical (right panel) component. From Figure 4.10(a) we observe that a decrease in the amplitude for both the component of Rayleigh wave after crossing the city can be inferred in the presence of city as compared to when there is no city. There is around 42.65 % and 58.97 % decrease in amplitude of horizontal and vertical component of Rayleigh wave at the recording station after interacting with the 30 RC building blocks of city. There is an increase of duration of ground motion in the case of response of the city. These extra phases may be due to the vibrations of the individual RC buildings blocks of the city. The vibrating blocks may release their energy to the earth in the form of body and the surface waves. Similarly, the left and right panels of Figure 4.10(b) show the comparison of spectra of the horizontal and vertical components of the response of the site-city model at the recording station with that in the absence of city. An analysis of Figure 4.10(b) shows drops in the spectra corresponding to the different modes of the flexural and longitudinal vibrations of the building blocks. These drops may be arising due to the phase difference (out of phase) of $\pi$ between the waves released by the building blocks as compared to the free field ground motion in the absence of city.

The left and right panels of Figure 4.10(c) show the spectral ratio of the horizontal and vertical components of the free field motion corresponding to with and without city in the model. An analysis of Figure 4.10(c) shows spectral ratio drops corresponding to the different modes of flexural and longitudinal vibrations of the building blocks Value of spectral ratio drop corresponding to the fundamental longitudinal mode of vibration of building blocks is the largest one. These spectral ratio drops for both the component of Rayleigh wave may be arising due to the signal released by the buildings which are out of phase to that of the incident Rayleigh waves. Further, the observed continuous increase of drop of spectral ratio with an increase of frequency may be due to the background scattering. In this case when impedance contrast is equal to one, we a get a band gap of 1.8Hz-3.5Hz.

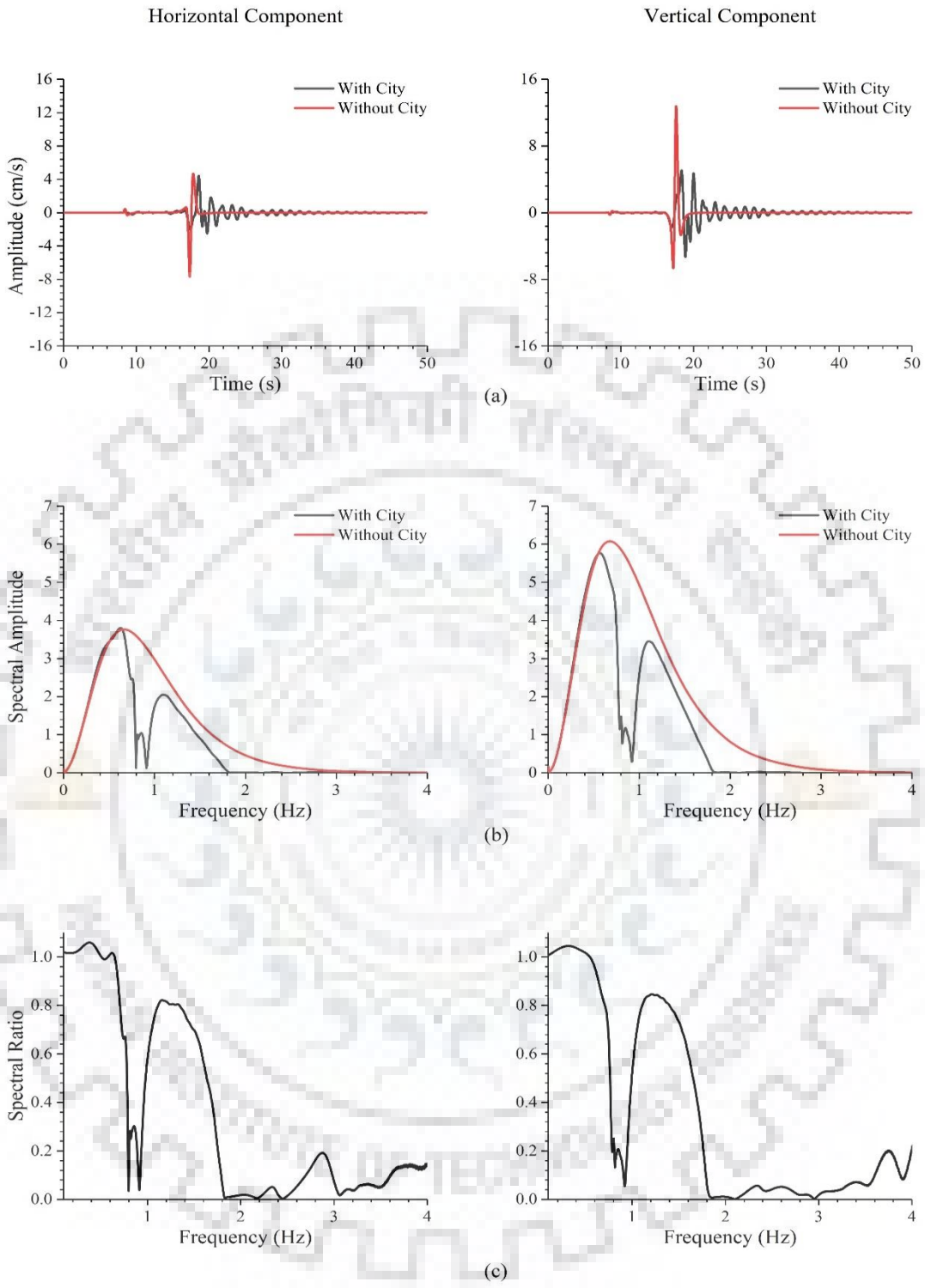


**Figure 4.10** (a) Comparison of responses of Rayleigh wave at (b) comparison of spectra (c) spectral ratios for the horizontal and vertical components of Rayleigh wave

## 4.4 Role of impedance contrast in meta-structure effect

In order to infer whether building blocks of the city (which may act as a sub-wavelength resonators) can develop a band-gap, the computed spectral ratio of responses corresponding to with and without city in the model needs further analysis. An analysis of Figure 4.6 shows the increase of spectral ratio drops at different flexural and longitudinal modes of vibrations of the RC-buildings with the decrease of IC between the building block and the underlying half-space. The spectral ratio drops at the longitudinal modes of vibrations are much larger than the flexural modes of vibrations of the building blocks. It is interesting to note that there is widening of the spectral ratio drops with the decrease of impedance contrast and the increase of modes of vibrations for longitudinal modes of vibration. In contrast to this, there is no widening of the spectral ratio drop at the fundamental flexural mode with the decrease of impedance contrast.

For example, there is a band-gap of width 1.8-3.2 Hz in the case of ICRC1 model, wherein impedance contrast is 2.33 and this band gap will further increases to 1.8-3.5 Hz for longitudinal modes when impedance contrast decreases to 1.02 This finding corroborates with the findings of Colombi et al. (2016), wherein a development of a frequency band-gap has been reported due to the interaction of trees of a forest with the Rayleigh waves which absorbs the energy of Rayleigh wave corresponding different longitudinal and flexural modes of vibrations and causes delays release of energy to the ground in the form of body waves and surface waves which are out of phases with incident Rayleigh wave.

## 4.5 Summary

The analysis of the Rayleigh wave responses of the city made-up of 30 RC-buildings reveals that the buildings of the city are acting as an insulator for the Rayleigh waves. There is an increase of insulating effect with a decrease of impedance contrast between the RC-buildings and the underlying half-space. The insulating effects of the 29 RC-buildings has caused around 71.53, 53.41%, 50.32%, 35.67%, and 20.89% for horizontal component and 52.44%, 46.48%, 34.35%, 18.62%, and 11.72% for vertical component, reduction of amplitude at the top of $30^{th}$ RC-building in the ICRC1 to ICRC5 site-city models, respectively. It is inferred that the building blocks may act as a meta-structure when the impedance contrast between the building blocks and the

underlying half-space is less than 10 and can create a large frequency band-gaps at their different longitudinal modes of vibrations (Colombi et al., 2016) and width of spectral ratio further increases to 1.8-3.5 Hz for longitudinal modes and also there is a slight widening of spectral ratio corresponding to flexural modes when impedance contrast decreases to 1.02.

# CHAPTER 5
# CONCLUSIONS

The analysis of simulated Rayleigh wave responses of the two cities made-up of 30 RC-buildings and 30 steel-buildings with 5-impedances in the underlying rock/sediment deposit revealed that the city is acting as an insulator for the Rayleigh waves. Further, this insulating effect on the Rayleigh wave is increasing with the decrease of impedance contrast between the buildings of the city and the underlying rock/sediment. It is concluded that the insulating effects of city is highly beneficial for the buildings falling in the end of city since there is very large reduction of response of the building corresponding to the longitudinal resonance frequency of the buildings which are ahead the building under consideration for dynamic analysis. The obtained insulating effects of steel-buildings is lesser than the RC-buildings.

The spectral ratio of Rayleigh wave responses recorded at free surface after crossing the city corresponding to with and without city in the model revealed a wide band-gap centered at the longitudinal modes of vibrations of the RC- and steel-buildings when impedance contrast is less than 15. Further, the width of this band-gap is increasing with further decrease of impedance contrast. However, it appears that the observed spectral ratio drops at the different flexural and longitudinal modes of vibrations of the RC- and steel-buildings in the cases of IC lesser than 15 are mainly due the vibrations of the building. Since, signals (body/Rayleigh waves) generated by the vibrating buildings are is out of phase with the Rayleigh wave at the recording station. Further, there is increase of spectral ratio drops with the decrease of IC in this case also. So, the development of band-gap and increase of width of the developed band-gaps with decrease of IC is an unexpected response of the city when IC is less 15. It may be inferred that buildings of the city are acting as a sub-wavelength resonator when IC is less than 15 and are violently vibrating through resonance scattering (Colombi et al., 2016). Finally, it may be concluded that the buildings of the city are acting as a meta-structure when the IC is less than around 15 and the meta-structure effects of the RC-building on the building response and the free field motion is more than that of the steel-building.

The seismologists and earthquake engineers bother a lot for the effects of 30 m sediment deposit during the prediction of seismic hazard. Now, question arise why not to bother for the buildings with heights exceeding 30 m and falling in the path of high frequency Rayleigh waves with large amplitude caused by the shallow earthquakes (Narayan and Kumar, 2010). Based on the obtained level of insulating and meta-structure effects on the building response and the free field motion, it is recommended to consider the insulating and meta-structure effects of a buildings falling in the path of Rayleigh waves during the estimation of seismic hazard in the epicentral zone of shallow earthquakes.

# REFERENCES


1. Bard, P. Y., Chazelas, J. L., Guéguen, P., Kham, M., and Semblat, J. F. (2005). "Site–city interaction. Assessing and Managing Earthquake Risk." (Geo-Scientific and Engineering Knowledge for Earthquake Risk Mitigation: Developments, Tools and Techniques), Oliveira CS, Roca A, Goula X Editors.
2. Colombi, A., Colquitt, D., Roux, P., Guenneau, S., and Craster, R. V. (2016a). "A seismic metamaterial: The resonant metawedge." *Scientific reports*, 6, 27717.
3. Colombi, A., Roux, P., Guenneau, S., Gueguen, P., and Craster, R. V. (2016b). "Forests as a natural seismic metamaterial: Rayleigh wave bandgaps induced by local resonances." *Scientific reports*, 6, 19238.
4. Emmerich, H., and Korn, M. (1987). "Incorporation of attenuation into time-domain computations of seismic wave fields." *Geophysics*, 52, 1252-1264.
5. Goffaux, C., Sánchez-Dehesa, J., Yeyati, A. L., Lambin, P., Khelif, A., Vasseur, J. O., and Djafari-Rouhani, B. (2002). "Evidence of Fano-like interference phenomena in locally resonant materials." *Physical review letters*, 88(22), 225502.
6. IS: 1893 (Part-1):2016. Criteria for Earthquake Resistant Design of structures. Part 1: General Provision and Buildings, Bureau of Indian Standards, New Delhi.
7. Israeli, M., and Orszag, S. A. (1981). "Approximation of radiation boundary conditions." *Journal of computational physics*, 41(1), 115-135.
8. Kham, M., Semblat, J. F., Bard, P. Y., and Dangla, P. (2006). "Seismic site–city interaction: main governing phenomena through simplified numerical models." *Bulletin of the Seismological Society of America*, 96(5), 1934-1951.
9. Kristek, J., and Moczo, P. (2003). "Seismic-wave propagation in viscoelastic media with material discontinuities A 3D fourth-order staggered-grid finite-difference modeling." *Bulletin of the Seismological Society of America*, 93(5), 2273-2280.
10. Kumar, N. and Narayan, J.P (2015). "Effect of SCI and polarization of the incident wave on the transfer function and fundamental frequency of the structure." *Natural Hazards*, 75(2). (under review)
11. Kumar, N., and Narayan, J. P. (2017). "Quantification of site–city interaction effects on the response of structure under double resonance condition." *Geophysical Journal International*, 212(1), 422-441.
12. Merritt, R. G., and Housner, G. W. (1954). "Effect of foundation compliance on earthquake stresses in multistory buildings." *Bulletin of the Seismological Society of America*, 44(4), 551-569.
13. Michel, C., & Gueguen, P. (2018). "Interpretation of the velocity measured in buildings by seismic interferometry based on Timoshenko beam theory under weak and moderate motion. "*Soil Dynamics and Earthquake Engineering*, 104, 131-142.

14. Michel, C., Guéguen, P. and Bard, P.Y., 2008. "Dynamic parameters of structures extracted from ambient vibration measurements: An aid for the seismic vulnerability assessment of existing buildings in moderate seismic hazard regions." *Soil dynamics and earthquake engineering*, 28(8), 593-604.

15. Narayan, J. P., and Kumar, S. (2008). "A fourth order accurate SH-wave staggered grid finite-difference algorithm with variable grid size and VGR-stress imaging technique." *Pure and Applied Geophysics*, 165(2), 271-294.

16. Narayan, J. P., and Kumar, S. (2010). "Study of effects of focal depth on the characteristics of Rayleigh waves using finite difference method." *Acta Geophysica*, 58(4), 624-644.

17. Narayan, J. P., and Kumar, V. (2013). "A fourth-order accurate finite-difference program for the simulation of SH-wave propagation in heterogeneous viscoelastic medium." *Geofizika*, 30(2), 173-189.

18. Narayan, J. P., and Kumar, V. (2014). "P-SV wave time-domain finite-difference algorithm with realistic damping and a combined study of effects of sediment rheology and basement focusing." *Acta Geophys*, 62(3), 1214-1245.

19. Narayan, J. P., and Kumar, V. (2014). "P-SV wave time-domain finite-difference algorithm with realistic damping and a combined study of effects of sediment rheology and basement focusing." *Acta Geophys*, 62(3), 1214-1245.

20. Pendry, J. B., Holden, A. J., Robbins, D. J., & Stewart, W. J. (1999). "Magnetism from conductors and enhanced nonlinear phenomena." *IEEE transactions on microwave theory and techniques*, 47(11), 2075-2084.

21. Sahar, D., and Narayan, J. P. (2016). "Quantification of modification of ground motion due to urbanization in a 3D basin using viscoelastic finite-difference modelling." *Natural Hazards*, 81(2), 779-806.

22. Sahar, D., Narayan, J. P., and Kumar, N. (2015). "Study of role of basin shape in the site–city interaction effects on the ground motion characteristics." *Natural Hazards*, 75(2), 1167-1186.

23. Savage, W. Z. (2004). "An exact solution for effects of topography on free Rayleigh waves." *Bulletin of the Seismological Society of America*, 94(5), 1706-1727.

24. Semblat, J. F., Kham, M., and Bard, P. Y. (2008). "Seismic-wave propagation in alluvial basins and influence of site-city interaction." *Bulletin of the Seismological Society of America*, 98(6), 2665-2678.

25. Tsakmakidis, K. L., Boardman, A. D., & Hess, O. (2007). "'Trapped rainbow' storage of light in metamaterials." *Nature*, 450(7168), 397.

26. Veselago, V. G. (1968). "Reviews of Topical Problems: The Electrodynamics of Substances with Simultaneously Negative Values of epsilon and mu." *Soviet Physics Uspekhi*, 10*(4)*, 509.

27. Wirgin, A., and Bard, P. Y. (1996). “Effects of buildings on the duration and amplitude of ground motion in Mexico City.” *Bulletin of the Seismological Society of America,* 86(3), 914-920.